

DnaA and the timing of chromosome replication in *Escherichia coli* as a function of growth rate

Matthew AA Grant¹, Chiara Saggioro², Ulisse Ferrari³, Bruno Bassetti^{4,5}, Bianca Sclavi² and Marco Cosentino Lagomarsino^{*6,7,4}

¹ BSS Group, Department of Physics, University of Cambridge, JJ Thomson Avenue, Cambridge, CB3 0HE, UK

² LBPA, UMR 8113 du CNRS, Ecole Normale Supérieure de Cachan, 61 Avenue du Président Wilson, 94235 CACHAN, France

³ Dip. Fisica, Università "Sapienza", and IPCF-CNR, UOS Roma Piazzale A. Moro 2, I-00185, Rome, Italy

⁴ Università degli Studi di Milano, Dip. Fisica. Via Celoria 16, 20133 Milano, Italy

⁵ I.N.F.N. Milano, Italy

⁶ Génophysique / Genomic Physics Group, UMR7238 CNRS "Microorganism Genomics"

⁷ University Pierre et Marie Curie, 15 rue de l'École de Médecine, 75006 Paris, France

Email: Matthew AA Grant - maag2@cam.ac.uk; Chiara Saggioro - csaggior@lbpa.ens-cachan.fr ; Ulisse Ferrari - ulisse.ferrari@gmail.com; Bruno Bassetti - Bruno.Bassetti@mi.infn.it; Bianca Sclavi - sclavi@lbpa.ens-cachan.fr; Marco Cosentino Lagomarsino* - marco.cosentino-lagomarsino@upmc.fr;

*Corresponding author

Abstract

Background: In *Escherichia coli*, overlapping rounds of DNA replication allow the bacteria to double in faster times than the time required to copy the genome. The precise timing of initiation of DNA replication is determined by a regulatory circuit that depends on the binding of a critical number of ATP-bound DnaA proteins at the origin of replication, resulting in the melting of the DNA and the assembly of the replication complex. The synthesis of DnaA in the cell is controlled by a growth-rate dependent, negatively autoregulated gene found near the origin of replication. Both the regulatory and initiation activity of DnaA depend on its nucleotide bound state and its availability.

Results: In order to investigate the contributions of the different regulatory processes to the timing of initiation of DNA replication at varying growth rates, we formulate a minimal quantitative model of the initiator circuit that includes the key ingredients known to regulate the activity of the DnaA protein. This model describes the average-cell oscillations in DnaA-ATP/DNA during the cell cycle, for varying growth rates. We evaluate the conditions under which this ratio attains the same threshold value at the time of initiation, independently of the growth rate.

Conclusions: We find that a quantitative description of replication initiation by DnaA must rely on the dependency of the basic parameters on growth rate, in order to account for the timing of initiation of DNA replication at different cell doubling times. We isolate two main possible scenarios for this, depending on the roles of DnaA autoregulation and DnaA ATP-hydrolysis regulatory process. One possibility is that the basal rate of regulatory inactivation by ATP hydrolysis must vary with growth rate. Alternatively, some parameters defining promoter activity need to be a function of the growth rate. In either case, the basal rate of gene expression needs to increase with the growth rate, in accordance with the known characteristics of the *dnaA* promoter. Furthermore, both inactivation and autorepression reduce the amplitude of the cell-cycle oscillations of DnaA-ATP/DNA.

Background

The coordination of DNA replication with cell division in *E. coli* is a classic problem of bacterial physiology [1]. It is connected with the control of the bacterial DNA replication and cell division cycle as a function of the growth rate, and it is an essential component for evolutionary adaptation to fast-growing conditions [2]. It is also a classic problem for biological modeling [3–7]. The main outstanding questions have to do with the characterization of the network of regulatory interactions by which cells determine the timing of initiation and limit it to once per cell cycle. The theoretical foundations for understanding chromosome replication initiation in *E. coli* were set by Cooper and Helmstetter [8], by showing that the time taken for a single chromosome to be replicated (*C* period) and the time period between completion of chromosome replication and the following cell division (*D* period) were approximately constant for a cell doubling time of less than one hour [9]. The same work also introduced the idea of overlapping rounds of chromosome replication, where a round of replication can be initiated while an existing round of replication is still proceeding (Figure 1). This mechanism allows *E. coli* to grow with a doubling time faster than the time required to copy its genome. The question then arises of how the cell determines when to initiate DNA replication and how this is coupled to the growth rate.

In 1968, Donachie calculated that the correct timing would be guaranteed by a constant ratio of the cell size at the moment of initiation (termed the ‘initiation mass’) and the number of *oriC* in the cell [10]. Direct measurements of this ratio or of the initiation mass from cell population are difficult. Thus, whether this ratio is effectively a constant

in cells with doubling times lower than one hour is to some extent an open question [11–14]. It was then proposed and debated that the amount of an initiating factor accumulating with the cell's mass could reach a threshold value resulting in activation of the origin(s). The DnaA protein has been shown to possess the basic characteristics necessary to act as such an initiator [15, 16]. Several monomers of DnaA bind cooperatively to *oriC* and induce DNA melting required for assembly of the replication forks [17–19]. Its level of expression increases with the growth rate [20] to result approximately in a constant amount of total DnaA per cell [16]. DnaA overexpression results in earlier initiation, and when it is depleted it results in delayed initiation [21, 22].

In addition, DnaA exists under two forms, ATP or ADP bound. The first is required for activation of the origin, thus it is usually called the active form [23]. After the replication of *oriC*, DnaA-ATP becomes converted to DnaA-ADP in a process known as 'RIDA' (Regulatory Inactivation of DnaA). RIDA is mediated by the Hda protein and the beta clamp subunit of the replisome and requires active replication forks [24, 25]. The hydrolysis of the ATP in a DNA-replication dependent manner decreases the activity of the protein after initiation has taken place, thus reducing the probability that a new initiation event will occur within the same cell cycle [24, 25]. At the same time the synthesis of new DNA creates new DnaA binding sites that can titrate DnaA from the origin [5, 26, 27].

Other processes can contribute to prevent reinitiation within the same cell cycle, such as the binding of the SeqA protein to the newly replicated, hemimethylated DNA [24, 28, 29]. It is believed that an “eclipse” period where reinitiation is not possible allows a buffer time for the other processes such as RIDA to take effect and thus for the levels of DnaA-ATP to decrease below the critical level for initiation. Several GATC sites are also found at the *dnaA* promoter but their effect on the timing of initiation remains to be established [30, 31]. Finally, a set of proteins have been shown to either inhibit or enhance the activity of DnaA at the origin. These are for the most part abundant nucleoid proteins such as FIS, HU and IHF, that may play a regulatory role as a function of changes in the growth phase [32].

DnaA-ATP binding to the origin must determine the timing of initiation for a range of growth rates and thus in the presence of increasing genome amounts (providing non-specific binding sites). Thus, the amount of DnaA-ATP per cell needs to increase with the decrease in doubling time. The *dnaA* gene is found next to the origin on the chromosome, resulting in the gene copy-number increasing with the number of origins. In addition, the expression of the *dnaA* gene is growth rate-dependent [16, 20, 33]. The *dnaA* promoter region contains multiple binding sites for DnaA with differential affinity and specificity for the ATP- and ADP-bound forms of the protein and has been shown to be autorepressed by DnaA-ATP but not DnaA-ADP [18]. Consistent with this negative autoregulation, the artificial addition of DnaA boxes in the cell results in an increase in gene expression [27, 34–36] and inhibition of the RIDA process or the presence of a mutant form of DnaA insensitive to RIDA (DnaAcos) results in a decrease in the level of

DnaA protein in the cell [37, 38]. Finally, DnaA is a transcription factor for a set of genes involved in regulation of DNA replication [19] and it could thus act as a reporter of the DNA replication state of the cell in order to maintain the correct stoichiometry of the DNA replication regulatory factors at varying growth rates and in response to perturbation to the movement of the replication forks [39].

It has previously been proposed that the presence of both autoregulation and RIDA contributes to increased robustness of the initiation regulatory network upon perturbations [24, 37]. In this work, we aim to determine the relative roles of these two regulatory processes in the control of the timing of initiation with changing growth rate. We begin from the elements provided by the Cooper and Helmstetter model in order to estimate the initiation time at different growth rates. The two main assumptions are that initiation of DNA replication is determined by a critical amount of DnaA-ATP per non-specific site on the genome and that this threshold value remains constant as a function of growth rate. On the other hand, the cellular and metabolic parameters can change with growth rate and have an impact on the DnaA circuit. In order to understand this, we use information from systematic studies of cellular changes with growth rate [40, 41]. Finally, the volume of the cell is assumed to be a less relevant background as a reservoir of DnaA-ATP than the number of non-specific binding sites on the DNA [42].

The resulting equations describe, via a continuous change in parameter values with growth rate, the oscillations in DnaA-ATP per non-specific site and the attainment of a constant threshold as a function of growth rate. This shows that the circuit performing the timing of replication initiation must encode subtle information on the bacterial physiological state through the growth rate dependence of the parameters. This analysis also allows us to define a few scenarios consistent with the available experimental knowledge and to make testable predictions on the relative roles of DnaA autorepression and of the RIDA process at different growth rates. We use this model to elucidate the reciprocal roles of the known factors affecting DnaA activity in *E. coli*, namely that DnaA expression is dependent on transcriptional autoregulation, and that its ATP-ase activity is coupled with the activity of the advancing replication forks (RIDA). The results show that a working system can still be produced in the absence of RIDA or DnaA autoregulation. Moreover, both RIDA and autorepression contribute to a decrease in the amplitude of the cell-cycle oscillations in DnaA-ATP. RIDA has a larger effect at the faster growth rates while negative regulation has a larger effect at slower growth.

Methods

Assumptions of the model. The model consists of a set of Ordinary Differential Equations (ODEs) describing DnaA-ATP production by the expression of the *dnaA* gene. It is built on two basic assumptions. The first is based on the evidence that a specific number of DnaA-ATP molecules need to bind on *oriC* in order to create a replication

bubble. Following the standard thermodynamic model of protein-DNA binding [42–44], the probability of this event is dependent on the number of DnaA-ATP molecules that are bound to the non-specific sites along the chromosome. These are low-affinity sites compared to titration sites, but the affinity is high enough so that the protein spends most of its time bound to the genome. These sequence-independent interactions are typical of DNA-binding proteins. As a consequence, the simplifying assumption is usually made [42] that the key molecular players (RNAP and TFs) are bound to the DNA either specifically or non-specifically. Simply stated, this is just an implementation of the known fact that DNA-binding proteins, besides binding tightly to their target sequences, are generally “sticky” for DNA, in a sequence-independent manner. This implies that the timing of DNA replication initiation in the cell is determined by the ratio DnaA-ATP to non-specific binding sites on DNA (which in turn must be proportional to the total DNA length of the chromosome(s) in the cell and effectively results in the computation of the amount of DNA per cell). Note that in this case the volume of the cell is not taken into consideration since it is not the change in concentration of DnaA or of DNA that determines the initiation time. The same will apply to the binding of DnaA and RNA polymerase to the *dnaA* promoter (see below). The second assumption is that at the time of initiation this ratio will be the same, independently of the growth rate and thus the number of origins.

We ask how the parameters of this model must vary in order for this assumption to hold in the range of doubling times between 20 and 60 minutes. In the absence of autoregulation, the only factor that contributes to a decrease in the ratio of DnaA-ATP to non-specific binding sites is the increase in DNA after DNA replication has begun. The complete model also includes the autoregulation of DnaA expression by DnaA binding to its own promoter [18] and DnaA-ATP transformation into DnaA-ADP through the RIDA process [37, 45]. It is assumed that this ODE description is applicable to a single average-cell on time scales shorter than the length of the cell cycle. This hypothesis could be challenged for the shortest observable doubling times, but the formulation of the model is dictated by maximizing simplicity. The values of the parameters (attributed to a specific value of the growth rate) are all taken or estimated from the available experimental measurements. They are shown in Table 1, together with the sources.

Formulation of the model

Timing of replication. We take into consideration the situation where the cell cycle repeats itself identically i.e. balanced, exponential growth. Following Cooper and Helmstetter, at a time $C + D$ after the initiation time, the cell divides, i.e. that time must be an integer multiple of the doubling time. Thus, if τ is the doubling time of the cell and X is the initiation time, then we must have

$$X + C + D = (n + 1)\tau , \tag{1}$$

where n is the integer number of times that τ divides $C + D$. n can be viewed as the number of overlapping rounds of replication, and 2^n is the number of origins. Thus, this equation reflects the phenomenon of overlapping replication rounds. Figure 1 shows how X varies with the doubling time (τ) of the cell. Defining Y as the time at which the chromosome completes replication, we have

$$Y = \tau - D. \quad (2)$$

Promoter term. The activity of the *dnaA* promoter is the source term for DnaA-ATP. We describe it by the standard thermodynamic model first used by Shea and Ackers [42–44]. We denote the promoter term (the number of DnaA-ATP synthesised per unit time) as Q , the number of non-specific binding sites on the chromosome as N_{NS} and the number of RNA polymerase (RNAP) molecules as P . Furthermore, we denote the number of DnaA-ATP molecules as A_- . We then use the assumption that the number of non-specific binding sites is proportional to the length of DNA in the cell (which we write as Λ), i.e. $\Lambda = \kappa N_{NS}$.

Thus the expression for the rate of transcription at the *dnaA* promoter can be written as (see Additional File 1, Section 2)

$$Q = \frac{k_A \Theta}{1 + c_1 \frac{\Lambda}{P} + c_2 \frac{A_-}{P}} \quad (3)$$

where k_A is the basal rate of transcription of the *dnaA* promoter, $\Theta(t, \tau)$ is the number of *dnaA* promoters (and genes) in a given cell at a given time, and the remaining factor is the probability of RNAP binding to the promoter. The parameters c_1 and c_2 depend on the binding energies $\Delta\epsilon_{pd}$ and $\Delta\epsilon_{ad}$ of RNAP and A_- respectively to their promoter binding sites. The binding energies are determined from the ratio of specific vs non-specific binding affinities.

$$\begin{aligned} c_1 &= \frac{e^{\Delta\epsilon_{pd}/k_B T}}{\kappa} \\ c_2 &= e^{(\Delta\epsilon_{pd} - \Delta\epsilon_{ad})/k_B T}. \end{aligned} \quad (4)$$

where the exponential terms are Boltzmann weights. $c_2 = 0$ if the promoter is not autorepressed. A version of the promoter where DnaA binding to its sites is cooperative is described in Additional File 1.

RIDA term. This term reflects the number of DnaA-ATP molecules that are converted to DnaA-ADP molecules per unit time by the RIDA process. As discussed in the introduction, RIDA is a process that takes place at the replication forks during DNA synthesis. We assume that the rate of conversion k_R takes the same value at each replication fork. The number of pairs of replication forks at a given time, $\mathcal{F}(t)$, depends on which of X and Y is larger.

For $X < Y$:

$$\mathcal{F}(t) = \begin{cases} 2^n - 1 & \text{if } 0 < t < X \\ 2 \cdot 2^n - 1 & \text{if } X < t < Y \\ 2(2^n - 1) & \text{if } Y < t < \tau \end{cases} \quad (5)$$

and for $X > Y$:

$$\mathcal{F}(t) = \begin{cases} 2^n - 1 & \text{if } 0 < t < Y \\ 2^n - 2 & \text{if } Y < t < X \\ 2(2^n - 1) & \text{if } X < t < \tau \end{cases} \quad (6)$$

(note that this equation is intrinsically discrete since it relates to the physical number of replication forks) and so the conversion from DnaA-ATP to DnaA-ADP takes place at a rate

$$k_R \mathcal{F}(t). \quad (7)$$

This leads to the following differential equations for DnaA-ATP (denoted A_-) and DnaA-ADP (denoted A_+)

$$\frac{\partial A_-}{\partial t} = \frac{k_A \Theta}{1 + c_1 \frac{\Lambda}{P} + c_2 \frac{A_-}{P}} - k_R \mathcal{F} \quad (8)$$

$$\frac{\partial A_+}{\partial t} = k_R \mathcal{F}. \quad (9)$$

Term for the growth of the chromosome. The growth of the chromosome is controlled by the replication forks.

Defining the rate of DNA synthesis of each pair of replication forks as k_Λ , we can write

$$\frac{\partial \Lambda}{\partial t} = k_\Lambda \mathcal{F}. \quad (10)$$

Assuming that k_Λ is constant, and normalizing so that $\Lambda = 1$ is the length of one full chromosome, we have

$$k_\Lambda = 1/C.$$

Main equation. Figure 2 summarizes the ingredients of the model. Defining $r = \frac{A_-}{\Lambda}$ and combining (8) and (10) we obtain the equation

$$\frac{\partial r}{\partial t} = \frac{1}{\Lambda} \left(\frac{\Theta k_A}{1 + c_1 \frac{\Lambda}{P} + c_2 \frac{\Lambda}{P} r} - (k_R + r k_\Lambda) \mathcal{F} \right). \quad (11)$$

This equation describes the dynamics of the variable $r = \frac{A_-}{\Lambda}$ which we suggest is a suitable candidate for the initiation potential since a specific number of DnaA-ATP molecules is needed to be available to bind to the origin in order to induce DNA melting, as described above. Note that usually such dynamic equations are written in terms of volume, thinking of averages over cell populations on time-scales longer than a cell cycle. We assume that the (time-varying) background of genomic binding sites is the relevant variable in a Shea-Ackers type model, extending to a single cell cycle the approach normally used for longer time scales [42–44]. We also assume that the volume can

be treated as a weak perturbation, which we neglect here. In other words, the various molecules of interest (RNA Polymerase, DnaA) are partitioned between the specific and non-specific binding sites on the chromosome. Furthermore, the most important factor that determines the probability of binding to a given promoter is the absolute number of protein molecules relative to the absolute number of these binding sites, rather than the amount of protein per cell volume, which in comparison does not change significantly, and it can thus be neglected to a good approximation. Thus, this assumption means that one need not track the volume of the cell, only the number of non-specific binding sites in the cell at a given time. This idea is discussed further in Additional File 1, Section 2. Here we assume that the initiation potential, r , always reaches the same value at $t = X$ independently of the growth rate and we ask how the parameters of this model must vary in order for this assumption to hold in the range of doubling times between 20 and 60 minutes. In the following, we will first establish that such a constant threshold cannot be obtained by a model with fixed parameters and then study the possible scenarios where different subsets of parameters are allowed to vary.

Main Assumptions. The model relies on the following further assumptions [24]: (i) All newly synthesised DnaA is immediately bound to ATP, due to the relative abundance of ATP in the cell compared to ADP and the high affinity of DnaA for ATP. (ii) DnaA-ADP is only created by conversion from DnaA-ATP by the RIDA process, when it is present. (iii) The probability of DnaA being bound to its sites at the origin or on the promoter, in the case of the presence of autorepression, is given by its thermodynamic equilibrium value. The same assumption holds for the binding of RNA polymerase to a particular promoter. This means that we assume that the rate for transcription initiation is much slower than the rates for RNAP binding and unbinding from the promoter. (iv) The rate of *dnaA* gene expression is proportional to the equilibrium probability that RNAP is bound to the *dnaA* promoter. (v) We do not consider translation directly and thus there is no time delay from transcription to protein production since the addition of this feature did not affect the result of the model (see Results). (vi) The number of non-specific binding sites on the DNA in each cell for both RNAP and DnaA is proportional to the total length of DNA in the cell [46]. (vii) The number of RNAP molecules in the cell, P , grows exponentially from cell birth to cell division, corresponding to the hypothesis of constant concentration and exponentially growing cell size [47]. A linear growth can also be used, however the dynamics of the model do not differ significantly between these two cases.

Numerical integration. The non-linearity of the main equation (11) necessitates the use of a numerical method of integration. We used a custom C++ implementation of the fourth-order Runge-Kutta method. The equation was integrated for values of the cell doubling time, τ , in the range $21\text{mins} \leq \tau \leq 60\text{mins}$.

In order to test for the constant threshold condition, a transformation was performed by integrating the equation for

$\tau = 21$ mins and using the value of r at initiation $t = X$ as the imposed threshold for the other values of the doubling time. Thus it was important to estimate, to a good degree of accuracy, values for the parameters at a doubling time of 21 mins. These values appear in Table 1. The parameter values are either taken to be constant (independent of cell doubling time) or are allowed to change and obtained as a consequence of the transformation (see Table 2 for whether a parameter is constant or allowed to vary in a given situation).

Results

A fixed set of parameters gives a varying initiation threshold with increasing growth rate.

We first describe the behaviour of the model with a fixed parameter set. The ratio $r = \frac{A}{\Lambda}$ increases from the time of birth of the new cell. This can be interpreted as the accumulation of the ‘initiation potential’. At initiation ($t = X$), r peaks (at the ‘initiation potential’ threshold) and then falls again due to the increase in the number of non-specific binding sites. When including the RIDA process, the total RIDA rate also increases following initiation, due to the higher number of active replication forks, contributing to the decrease in the initiation potential. However, the value of r at $t = X$ varies for the different values of the doubling time τ (Figure 3A). Thus, it appears that this model, with fixed parameters, cannot give a constant threshold that is reached at initiation in the range of growth rates considered here.

This fact naturally leads us to consider a model in which the parameters are able to vary with growth rate.

Biologically, this is a natural requirement, as one may well expect from previous observations of the change in cellular components as a function of growth rate [40, 41, 48, 49].

A constant threshold condition implies alternative scenarios of growth-rate dependency in the circuit architecture

The condition of a constant DnaA-ATP/DNA threshold at the time of initiation can be imposed by performing a mathematical transformation on the model and verifying the implications of this for the values of the parameters. The mathematical details of this transformation can be found in Additional File 1, Section 3. The transformation yields a fixed threshold in r that is reached at initiation. This can be seen upon comparing the plots in Figure 3A and B. In the latter, the value of $r(X)$ is now the same at initiation for every cell doubling time. We estimate all initial values of the parameters from the literature (Table 1) and then we allow some of the parameters to change during the transformation. Thus, the transformation procedure imposes a decision on which parameters to fix and which to allow to change. This determines different scenarios, as illustrated in Figures 4 and 5 and also summarised in Table 2 (see also Additional File 1, Section 3 and Additional File 1, Figure A1). These plots explicitly show the required parameter changes at varying growth rates.

1. In the first scenario, the RIDA rate (per replication fork), k_R , is chosen to remain independent of growth rate, and the other parameters are allowed to change. The transformation fixes the scaling of k_A with growth rate, and provides an equation that c_1 and P must satisfy. Since the constraints reduce to one equation with two unknowns, there is a set of possible solutions for c_1 and P , and the scenario is underconstrained (see Additional File 1, Section 3). One possibility is to fix one of the parameters to a particular trend, in turn determining the second parameter, determining different subscenarios (Additional File 1, Figure A1).
 - (a) In the first of these sub-scenarios, 1a, the variation in the number of non-specifically bound RNAP in the cell, P , with growth rate is fixed *a priori* by imposing the trend of a previous study [41], which partitions RNAP into different classes, the RNAP bound on promoters and non-specifically bound, and determines the dependence of this partition with growth rate, (see Figure 4A). Imposing this trend determines the values for the binding affinity of RNAP to the promoter, which must vary with growth rate (Additional File 1, Section 3).
 - (b) In sub-scenario 1b, the binding affinity of RNAP to the *dnaA* promoter is chosen to remain independent of growth rate. Fixing this parameter constrains the remaining equation, thereby imposing a particular dependence on growth rate of the number of non-specifically bound RNAP, P , which turns out to be compatible with ref. [41] (see Additional File 1, Section 3 and Figure 4A).
2. In scenario 2, the binding affinity of both RNAP to the *dnaA* promoter and of DnaA-ATP to its repression sites are chosen to remain independent of growth rate (in simulations, at the values shown in Table 1), while the basal rate of transcription from the *dnaA* promoter, k_A , the levels of free RNAP, P , and the RIDA rate (per replication fork), k_R are all permitted to vary from their original values (see Figures 4A and 5B). This scenario is also feasible in absence of autorepression.

In brief, two possible scenarios can result in a constant initiation threshold for the model. In the first, the binding affinity of DnaA-ATP to its repressor sites decreases with increasing cell doubling time and in the second the RIDA rate increases with cell doubling time. In both scenarios k_A (the basal transcription rate) must decrease with increasing cell doubling time. It is important to note that k_A , the basal *dnaA* transcription rate, needs to vary in all scenarios with growth rate. This term (and hence its variation) is independent from RNAP availability (our P term) and binding (our c_1 and c_2 terms). It describes how quickly RNAP moves through a gene when transcribing. The variation of this characteristic time with growth rate can be associated with variations in DNA supercoiling (see Discussion).

In absence of RIDA ($k_R = 0$) or autorepression ($c_2 = 0$), the transformation can still be performed. However, it implies that the ratio c_1/P should remain constant with growth rate. Since P varies [41], this means that c_1 (which, for example, could also vary through changes in supercoiling) would have to compensate exactly for the changes in P in order to keep a constant threshold. We have considered these further scenarios to be less probable, because they may result in a less robust control due to an unlikely fine-tuning of two parameters.

The resulting scenarios are compatible with available knowledge on RNAP availability and total DnaA expression

Given these scenarios, we have asked whether the predicted parameter variation with growth rate and the observables quantities produced by the model were compatible with the measurements and observations available in the literature. Starting from the dependency of available RNAP with growth rate, this is predicted and matched with available experimental data in ref. [41]. Scenario 1a assumes this dependency, and therefore automatically accounts for this observation. Figure 4A demonstrates how also scenarios 1b and 2 are broadly compatible with the results of Klumpp and Hwa [41] since the average levels of non-specifically bound RNA polymerase decrease with increasing doubling time in all cases.

We now turn to the changes in measured expression of DnaA (averaged over a population) with growth rate. This can be measured by a reporter gene technique. Figure 4B shows how the model predicts that the average expression of the *dnaA* gene should change with growth rate in all scenarios. This appears to be independent of the scenario chosen and is compatible with previous findings [20]. We have also performed our own measurements, using a GFP reporter of the *dnaA* promoter encoded on a plasmid (and normalizing the result for plasmid and gene copy number (Chiara Saggioro, Anne Olliver, Bianca Sclavi: Multiple levels of regulation in the growth rate dependence of DnaA expression, submitted), see also Additional File 1, Section 7), confirming this agreement (Figure 4B).

Finally, at fixed growth rate, in order to determine whether this model reflects the main features of the regulatory network in the cell, we reproduced some of the experimental perturbations described in the literature. One of these experiments changed the rate of RIDA by changing the level of expression of the gene encoding for the Hda protein [37], while others controlled the expression of DnaA independently of the *dnaA* promoter. We found that a constant threshold can be obtained upon a 10 fold change in the RIDA rate (Additional File 1, Figure A4). In order to determine how RIDA rate and autorepression strength influence the activity of DnaA-ATP within a cell cycle in the model, we have monitored the amplitude of the oscillations of the ratio DnaA-ATP:total genome length. The results show that increased autorepression contributes to a smaller amplitude of DnaA-ATP within the cell cycle (Additional File 1, Figure A2). A decrease in RIDA has the opposite effect, and is compensated for by an increase in

autorepression. In either case the inclusion of these additional control factors appears to result in smaller amplitude in the oscillation of DnaA-ATP and a smaller variation in the average amount of DnaA-ATP per cell as the growth rate is varied. This may be advantageous for the use of DnaA as a transcription factor whose activity is responsive to changes in the replication status of the cell, via the RIDA and titration effects.

Finally, once we obtained a set of parameters that satisfies the constant threshold constraint, we modified the RIDA rate while leaving the other parameters unchanged (Additional File 1, Figure A7), attempting to reproduce the effect of under or over expressing the Hda protein, as in the experiments by Riber *et al.* [37]. In our model, this results in a change of the threshold value as a function of growth rate, and more significantly at slow growth. At faster RIDA rate, the threshold value is higher at slow growth, while the opposite is observed when RIDA rate is decreased.

These compatibility tests give positive results, but do not allow us to distinguish between the two scenarios. We have explored the literature for tests of dependency of the RIDA rate with growth rate, and have found no evidence of this, which lead us to consider scenario 1, where the RIDA rate is constant as the main one.

Model Variants

In order to gain confidence that the conclusion (that the parameters need to vary with growth rate) is not a consequence of the restricted set of biological ingredients included in this model, we considered some additional model variants, including some of the known factors that may influence the timing of replication initiation.

1. **Delay in the synthesis of DnaA-ATP.** We introduced a delay, representing the time necessary to obtain an active DnaA molecule from the binding of the RNA polymerase to the *dnaA* promoter to the end of translation. This delay, however, does not produce a significant effect in imposing a DnaA-ATP threshold at initiation, suggesting that translation delay might not have a predominant role in controlling the timing of initiation (see Additional File 1, Figure A6B).
2. **Cooperativity of autorepression.** Cooperativity of autorepression affects the growth rate dependence of gene expression [41]. Additional File 1, Figure A6C shows by simulation that the presence of cooperativity alone cannot explain a constant threshold. Thus it is still necessary to impose a constant threshold on the model using a transformation such as that described in Additional File 1, Section 3. However, in general one cannot make a translation and scaling and keep the promoter in the same form (see also Additional File 1, Section 5), and the transformation itself poses complex constraints on the possible regulations. Thus, we decided to concentrate on the simpler non-cooperative model. Biologically, of the two high-affinity DnaA sites found at the *dnaA* promoter, one matches exactly the consensus sequence, and has a higher affinity than the other [18], suggesting

that at lower DnaA concentrations only one monomer could be bound. We have verified that the transformation is possible with a promoter that would fit this profile, i.e. of the form

$$Q = \frac{k_A \Theta}{1 + c_1 \frac{\Lambda}{P} \left(\frac{1 + \frac{r}{k_1} + \frac{r^2 \omega}{k_1 k_2}}{1 + \frac{r}{k_1}} \right)},$$

where the parameter ω represents the cooperativity, and where k_1 and k_2 are the binding affinities of the two DnaA binding sites, multiplied by the proportionality constant between Λ and N_{NS} . This description introduces two new parameters - the cooperativity and the binding affinity of the second binding site. Since these parameters appear in the equations describing the transformation that keeps the constant threshold, the scenarios become more underconstrained in a non-essential way. Thus, while a more realistic promoter model could be useful for future descriptions, we decided not to pursue it here.

3. **The *datA* locus and specific DnaA binding sites.** We considered the effect that the presence of the *datA* locus has on the model by introducing a site on the chromosome that binds up to 300 DnaA-ATP molecules immediately after initiation has taken place (since *datA* is close to the origin on the chromosome, it is copied soon after initiation). We included one *datA* site for each origin in the cell. The results indicate that the *datA* locus might indeed prevent further initiations in a given cell cycle, since it titrates large numbers of DnaA-ATP molecules, effectively preventing them from binding at the origin (see Additional File 1, Figure A6A). However, this variant of the model fails to achieve a constant DnaA-ATP threshold at initiation at different growth rates if all parameters are kept constant. One can speculate that the large increase in *datA* sites at faster growth rates would require a proportional increase in the rate of DnaA synthesis that cannot be solely provided by the increase in gene copy number. It must be also noted that the *datA* locus appears to be unnecessary to prevent reinitiation and limit initiation of to once per cell cycle [50]. Additionally, we considered the effect of the reported ≈ 300 binding sites distributed around the chromosome [51]. These high-affinity sites would sequester DnaA in a similar way as the *datA* locus, but proportionally to the genome amount, and thus effectively decrease its concentration. This is again insufficient to guarantee a constant initiation threshold and is equivalent to rescaling the RIDA rate (see Additional File 1, Section 6.2).
4. **The eclipse.** No constraint for the eclipse period [24,28–31] was included in this model. This proved not to be necessary, probably because there is no delay between the attainment of the threshold and the initiation of DNA replication, thus avoiding the possibility that there is an ‘overshoot’ of initiation potential before both RIDA and the increase of non-specific DNA can begin. On the other hand, the gene copy number immediately doubles upon initiation of DNA replication which results in a sudden increase in the number of DnaA-ATP

synthesized per unit time. However, this does not result in an increase in the initiation potential due to the corresponding increase in the number of replication forks and thus on the RIDA rate and the number of non-specific titrating sites.

5. **DnaA-ATP Recycling regions.** Genomic recycling regions catalyzing the reconversion of DnaA-ADP into DnaA-ATP [52] have been recently discovered. The quantitative contribution of this process is not clear, but within our framework it makes sense to ask how this would affect the initiation threshold, as this process is, roughly, a correction to RIDA. Precisely, assuming DnaA-ADP is not limiting, this would change the model by the substitution of k_R with $k_R - \rho\Lambda/\mathcal{F}$ where ρ is a fixed recycling rate. We verified that in the model this recycling term cannot by itself impose a constant threshold, while it can contribute to correcting quantitatively the effective RIDA rate (Additional File 1, Section 6.1).

Since none of these model variants qualitatively changes the behaviour of the model with respect to attaining a constant initiation threshold, they were not included in the minimal model formulation, in order to avoid confusion and proliferation of parameters. However, as shown by the variants explored above, the qualitative behaviour that the parameters of the model must vary with growth rate does not hold strictly for the minimal model only, but might be more general.

Discussion

Standard models of bacterial regulatory circuits were adapted to situations where the growth rate is fixed [42, 53].

The notion that these quantitative descriptions must account for bacterial physiology through the growth-rate dependent basic partitioning of the cell physico-chemical components is now entering the field of systems biology through a combination of new work [41, 48, 49, 54] and reconsideration of the classics [8, 40, 55].

The dependency of the basic parameters on growth rate can produce notable effects on a genetic circuit, and complicates the standard descriptions [56]. In our case, the task is more difficult, as the circuit under examination is active in *determining* some features of the bacterial physiology and not only affected by them. Furthermore, on the technical level, one must produce a time-dependent description the expression of DnaA over cell-cycles of a range of durations. Perhaps also for this reason, despite the fact that the regulation of DNA replication has been a subject of intense study for over 50 years [24, 57], many questions remain open. Given these obstacles, we have shown that, under a series of simplifying hypotheses, a consistent mean-field description for the DnaA / replication initiation circuit is possible with varying growth rate.

Our description includes the processes that are believed to be most important for initiation of replication [24]. In these respects, it is broadly compatible with previous modelling approaches [4–7]. Its originality lies in the minimality and in the attention given to growth-rate dependency. We focused on the minimal ingredients necessary in order for the basic tenet that the ratio DnaA-ATP/DNA attains a constant threshold at initiation to hold [58, 59]. The validity of this tenet is confirmed by the recent observations that initiation time is not affected by adding an extra origin on the chromosome [58] and on the compensatory mutations emerging in Hda mutants [59].

We have defined the DNA replication initiation potential, determining the (synchronous) timing of DNA replication, as the DnaA-ATP to DNA ratio, r . Molecular titration has been shown to result in ultrasensitive “all or none” responses [60], which further justifies using r as the threshold and could explain the synchrony of initiation in cells containing *oriC* minichromosomes [61]. We assume that its value at the time of initiation, $r(X)$, is independent of the specific growth rate. The amount of DnaA-ATP at the time of initiation thus needs to increase as a function of growth rate in order for $r(X)$ to remain constant as a function of doubling time, and we found that consequently, some of the model’s parameter values must be allowed to vary. This assumption has not been verified directly. On the other hand, we feel that our point of view would still be useful in case of a growth-rate dependent $r(X)$, as it is unlikely that this dependence would automatically match the dependence of all the other parameters.

We have defined two main scenarios in which different subsets of the parameters are allowed to change. In Scenario 1 the RIDA rate (per replication fork), k_R , is held constant as a function of growth rate, but the binding affinities of RNAP and DnaA-ATP to the DNA need to vary with growth rate (note that in addition, there are two technical sub-scenarios to Scenario 1 due to the possibility of either fixing the growth rate dependence of P , the number of available RNA polymerase molecules a priori to the trend of ref. [41] (Scenario 1a) or allowing it to be free (Scenario 1b)). In Scenario 2 the binding constants (c.f. c_1 and c_2) are independent of growth rate but the RIDA rate, k_R , must vary. We have verified that both scenarios are consistent with the experimentally tested predictions of RNAP availability with growth rate [41] and with previous measurements [20] and our own experimental evaluation of total DnaA expression (Chiara Saggioro, Anne Olliver, Bianca Sclavi: Multiple levels of regulation in the growth rate dependence of DnaA expression, submitted), and also with a number of “in silico mutations” inspired by the available literature [24, 37]. Thus, the scenarios appear as possibilities that are testable, but for the moment remain open. Note that the property that the initiation threshold holds constant with respect to growth rate changes *is not* related to the specific set of parameters we used, or any set of parameters. Our analysis shows that in general, for any fixed parameter set at a given growth rate, a transformation is necessary in order to keep the threshold constant while moving to another growth rate. In order to provide specific examples, we have produced plots in the style of those in Figure 5, with different curves corresponding to choosing different values of the initial input parameters. These

demonstrate that the qualitative behaviour of the transformation is independent of these parameters (Additional File 1, Figures A8, A9 and A10). This exercise is also important to show that the parameter changes with growth rate are not numerically negligible for empirically plausible parameters, so that the question of keeping the initiation threshold constant is not purely academic.

It is then interesting to ask which of these scenarios is more reasonable considering the known biological processes. We speculate that scenario 2 is less likely, since until now there is no evidence pointing to a possible change in the intrinsic RIDA rate as a function of growth rate. The DnaA-related protein Hda (Homologous to DnaA) mediates this process [57]. Experiments with mutants over- and underexpressing Hda [37], with corresponding increases and decreases in the RIDA rate, suggest a possible mechanism by which the k_R term in the equations could vary by a growth rate-dependent expression of the Hda gene. There may also be other, as yet unknown, factors that affect the growth rate dependence of the RIDA rate. Alternatively, we can speculate that the decrease in the rate of RIDA with growth rate could be caused effectively by the action of the reverse process of DnaA-ATP recycling by the recently discovered recycling regions [52]. Figure 5b shows that the RIDA rate should increase with cell cycle time and thus decrease with growth rate. This growth rate increase causes overlapping replication rounds, and thus higher chromosome copy number. Since more recycling regions are present there is more recycling, *i.e.* a decrease in the effective RIDA rate, compatibility with the requirement imposed by our results. However, considering explicitly this model variant, we find that the balancing recycling cannot by itself impose a constant threshold.

Conversely in scenario 1, the RIDA rate per replication fork is constant, and one has to rationalize the variation of the binding affinities. It seems possible that the binding affinities could change with growth rate through changes in supercoiling, in similar ways to those seen in Figure 5 and Additional File 1, Figure A5 [62,63]. The levels of average negative supercoiling are known to increase as the growth rate increases [64]. However, it makes sense to challenge the validity of the basic assumption that the ratio of DnaA-ATP to DNA at the time of initiation is constant. This model assumes that the affinity for DnaA-ATP binding to its own promoter can change with growth rate but its affinity for the origin does not. The first assumption mainly allows the model to change the magnitude of negative autoregulation as a function of growth rate, and it may indeed be explained by the changes in global cellular parameters such as negative supercoiling. We have considered how the activation threshold in the model (estimated in Additional File 1, Figure A11 and corresponding caption) would be affected if the binding affinity for DnaA to the origin would vary in the same way as its value at the dnaA promoter, required by Scenario 1, for a set of realistic parameters. We found that these changes in $r(X)$ are less than 10% over a wide range of growth rates, suggesting that this scenario might be robust. Indeed, the observed threshold is certainly approximately constant when compared to the untransformed case *i.e.* the different values of the ratio at $t = X$ shown in Figure 3A. More generally, the

initiation of DNA replication has been significantly simplified in this model; all it requires is a specific amount of available DnaA-ATP molecules. However we know that other factors, such as the binding of nucleoid proteins FIS, IHF, H-NS and HU, may contribute to the formation of an open complex at the origin. On the other hand, other recent results have shown that at slower growth (slower than the range considered here) the cell contains a greater average amount of DnaA-ATP per origin that results in initiation events that are independent of the novel synthesis of DnaA-ATP [65]. These results suggest that the regulation of the initiation process at the origin might indeed be dependent on the growth rate and that these changes still remain to be characterized quantitatively before they can be included in a theoretical model.

Interestingly, the basal rate of transcription of the *dnaA* gene, k_A must vary in both scenarios. Figure 5 shows that k_A decreases as the cells grow more slowly. This is what is expected from a promoter like the one of the *dnaA* gene that closely resembles ribosomal RNA promoters. This family of promoters have a GC-rich sequence at the transcription initiation site called a discriminator region. This region renders the activity of the promoter sensitive to the degree of negative supercoiling, which activates transcription by enhancing DNA melting, and leads to its inhibition by the accumulation of ppGpp at slower growth rates [66].

Conclusions

All things considered, we can say that perhaps our main result is that the determination of the timing of initiation by DnaA, besides relying on the known “architecture” comprising autorepression, RIDA and a number of other “dedicated” processes, can be understood only in its complex interplay with bacterial physiology (comprising DNA supercoiling, ppGpp, growth-rate dependent partitioning of molecular machinery, etc.)

Nevertheless, it makes sense to ask whether this model allows us to elucidate some features of the reciprocal role of RIDA and DnaA autorepression, its two main ingredients. Biologically, RIDA renders the control of DnaA-ATP dependent upon ongoing DNA replication, and thus results in an increase in DnaA-ATP when replication forks are blocked. Autorepression however probably plays a larger role in the absence of RIDA at slow growth, or in bacteria that do not have RIDA at all (such as *B. subtilis*, where DnaA titration at the replication fork seems to play an important role) [57]. The Hda protein and thus the RIDA process seems to be quite specific to the fast-growing *E. coli* bacterium and its close relatives in the *Enterobacteriaceae* (UniProtKB), suggesting that in other bacterial species this level of regulation may not be required and is replaced instead by protein degradation, e.g. in *Caulobacter* [67,68], or a high intrinsic ATPase activity of the protein, as in *Mycobacterium tuberculosis* [69]. We have verified that the model can work in the absence of autorepression or RIDA, but the tuning of the parameters to achieve a constant threshold is more “difficult”, in the sense that it requires more fine-tuning of the parameters, since

the ratio c_1/P should remain constant with growth rate. meaning that it is possible that a smaller range of growth rates would be accessible in these conditions. Moreover, in the model, increasing autorepression or RIDA rate results in a smaller amplitude of the oscillations of the ratio DnaA-ATP/DNA during the cell cycle, and in a smaller variation in the average amount of DnaA-ATP per cell as the growth rate is varied. This may be advantageous for the use of DnaA as a transcription factor which has to sense perturbations in the replication status of the cell at all growth rates.

Competing Interests

The authors declare that they have no competing interests.

Authors Contributions

MCL, BS, and BB designed research. MG, BB, MCL, UF, and CS performed research. MG, BS and MCL wrote the paper. All authors read and approved the final manuscript.

Acknowledgements

We are grateful to Matteo Osella, Rosalind Allen, Pietro Cicuta, Antonio Celani, Andrea Sportiello, Kunihiro Kaneko and Massimo Vergassola for useful discussions and feedback. The authors acknowledge support from the Human Frontier Science Program Organization (Grant RGY0069/2009-C) and from EPSRC.

References

1. Meselson M, Stahl FW: **The replication of DNA in *Escherichia coli***. *PNAS* 1968, **44**:671–682.
2. Rocha EPC: **The replication-related organization of bacterial genomes**. *Microbiology* 2004, **150**(Pt 6):1609–1627.
3. Sompayrac L, Maaloe O: **Autorepressor model for control of DNA replication**. *Nat New Biol* 1973, **241**(109):133–135.
4. Margalit H, Rosenberger RF, Grover NB: **Initiation of DNA replication in bacteria: analysis of an autorepressor control model**. *J Theor Biol* 1984, **111**:183–199.
5. Hansen FG, Christensen BB, Atlung T: **The initiator titration model: computer simulation of chromosome and minichromosome control**. *Research in Microbiology* 1991, **142**:161–167.
6. Browning S, Castellanos M, Shuler M: **Robust control of initiation of prokaryotic chromosome replication: essential consideration for a minimal cell**. *Biotechnology and Bioengineering* 2004, **88**:575–584.
7. Nilsson K, Ehrenberg M: **A novel mechanism for activator-controlled initiation of DNA replication that resolves the auto-regulation sequestration paradox**. In *Aspects of Physical Biology, Volume 752 of Lecture Notes in Physics*. Edited by G Franzese & M Rubi, Berlin Springer Verlag 2008:189–213.
8. Cooper S, Helmstetter C: **Chromosome replication and the division cycle of *Escherichia coli* B/r**. *Journal of Molecular Biology* 1968, **31**:519–540.
9. Michelsen O, Teixeira de Mattos MJ, Jensen PR, Hansen FG: **Precise determinations of C and D periods by flow cytometry in *Escherichia coli* K-12 and B/r**. *Microbiology* 2003, **149**(4):1001–1010.
10. Donachie W: **Relationships between cell size and time of initiation of DNA replication**. *Nature* 1968, **219**:1077–1079.
11. Wold S, Skarstad K, Steen HB, Stokke T, Boye E: **The initiation mass for DNA replication in *Escherichia coli* K-12 is dependent on growth rate**. *The EMBO Journal* 1994, **13**:2097–2102.

12. Cooper S: **Does the initiation mass for DNA replication in *Escherichia coli* vary with growth rate?** *MicroCorrespondence* 1997, **26**:1138–1141.
13. Boye E, Nordstrøm K: **Coupling the cell cycle to cell growth.** *EMBO Rep* 2003, **4**(8):757–760.
14. Bates D, Kleckner N: **Chromosome and replisome dynamics in *E. coli*: loss of sister cohesion triggers global chromosome movement and mediates chromosome segregation.** *Cell* 2005, **121**(6):899–911.
15. Løbner-Olesen A, Skarstad K, Hansen FG, von Meyenburg K, Boye E: **The DnaA protein determines the initiation mass of *Escherichia coli* K-12.** *Cell* 1989, **57**(5):881–889.
16. Hansen F, Atlung T, Braun R, Wright A, Hughes P, Kohiyama M: **Initiator (DnaA) protein concentration as a function of growth rate in *Escherichia coli* and *Salmonella typhimurium*.** *Journal of Bacteriology* 1991, **173**(16):5194–5199.
17. Kornberg A, Baker TA: *DNA replication - Second edition.* University Science Books 2005.
18. Speck C, Messer W: **Mechanism of origin unwinding: sequential binding of DnaA to double- and single-stranded DNA.** *The EMBO Journal* 2001, **20**:1469–1476.
19. Messer W: **The bacterial replication initiator DnaA. DnaA and *oriC*, the bacterial mode to initiate DNA replication.** *FEMS Microbiology Reviews* 2002, **26**:355–374.
20. Chiaramello AE, Zyskind JW: **Expression of *Escherichia coli* *dnaA* and *mioC* genes as a function of growth rate.** *Journal of Bacteriology* 1989, **171**:4272–4280.
21. Atlung TA, Løbner-Olesen A, Hansen FG: **Over-production of DnaA protein stimulates initiation of chromosome and minichromosome replication in *E. coli*.** *Molecular Genomics and Genetics* 1987, **206**:51–59.
22. Bremer H, Churchward G: **Initiation of chromosome replication in *Escherichia coli* after induction of *dnaA* gene expression from a *lac* promoter.** *J Bacteriol* 1985, **164**(2):922–924.
23. Sekimizu K, Bramhill D, Kornberg A: **Sequential early stages in the *in vitro* initiation of replication at the origin of the *Escherichia coli* chromosome.** *The Journal of Biological Chemistry* 1988, **263**:7124–7130.
24. Donachie W, Blakely G: **Coupling the initiation of chromosome replication to cell size in *Escherichia coli*.** *Current Opinion in Microbiology* 2003, **6**:146–150.
25. Kurokawa K, Nishida S, Emoto A, Sekimizu K, Katayama T: **Replication cycle-coordinated change of the adenine nucleotide-bound forms of DnaA protein in *Escherichia coli*.** *The EMBO Journal* 1999, **18**:6642–6652.
26. Ogawa T, Yamada Y, Kuroda T, Kishi T, Moriya S: **The *datA* locus predominantly contributes to the initiator titration mechanism in the control of replication initiation in *Escherichia coli*.** *Molecular Microbiology* 2002, **44**(5):1367–1375.
27. Morigen, Boye E, Skarstad K, Løbner-Olesen A: **Regulation of chromosomal replication by DnaA protein availability in *Escherichia coli*: effects of the *datA* region.** *Biochimica et Biophysica Acta* 2001, **1521**:73–80.
28. von Freiesleben U, Krekling MA, Hansen FG, Løbner-Olesen A: **The eclipse period of *Escherichia coli*.** *The EMBO Journal* 2000, **19**:6240–6248.
29. Boye E, Stokke T, Kleckner N, Skarstad K: **Coordinating DNA replication initiation with cell growth: differential roles for DnaA and SeqA proteins.** *PNAS* 1996, **93**:12206–12211.
30. Zaritsky A, RA Vischer N: **Changes of initiation mass and cell dimensions by the ‘eclipse’.** *Molecular microbiology* 2007, **63**:15–21.
31. Kedar GC, Ozcan F, Guzmán EC, Smith DW, Newman VG, Zyskind JW: **Role of DNA methylation at GATC sites in the *dnaA* promoter, *dnaAp2*.** *Journal of Molecular Microbiology and Biotechnology* 2000, **2**:301–310.
32. Polaczek P, Kwan K, Liberles DA, Campbell JL: **Role of architectural elements in combinatorial regulation of initiation of DNA replication in *Escherichia coli*.** *Mol Microbiol* 1997, **26**(2):261–275.
33. Polaczek P, Wright A: **Regulation of expression of the *dnaA* gene in *Escherichia coli*: role of the two promoters and the DnaA box.** *New Biol* 1990, **2**(6):574–582.
34. Hansen FG, Koefoed S, Sorensen L, Atlung T: **Titration of DnaA protein by *oriC* DnaA-boxes increases *dnaA* gene expression in *Escherichia coli*.** *The EMBO Journal* 1987, **6**:255–258.
35. Christensen BB, Atlung T, Hansen FG: **DnaA boxes are important elements in setting the initiation mass of *Escherichia coli*.** *Journal of Bacteriology* 1999, **181**:2683–2688.
36. Kitagawa R, Mitsuki H, Okazaki T, Ogawa T: **A novel DnaA protein-binding site at 94.7 min on the *Escherichia coli* chromosome.** *Molecular Microbiology* 1996, **19**:1137–1147.

37. Riber L, Olsson JA, Jensen RB, Skovgaard O, Dasgupta S, Marinus MG, Løbner-Olesen A: **Hda-mediated inactivation of the DnaA protein and *dnaA* gene autoregulation act in concert to ensure homeostatic maintenance of the *Escherichia coli* chromosome.** *Genes and Development* 2006, **20**:2121–2134.
38. Katayama T, Kornberg A: **Hyperactive initiation of chromosomal replication in vivo and in vitro by a mutant initiator protein, DnaAcos, of *Escherichia coli*.** *J Biol Chem* 1994, **269**(17):12698–12703.
39. Olliver A, Saggiaro C, Herrick J, Sclavi B: **DnaA-ATP acts as a molecular switch to control levels of ribonucleotide reductase expression in *Escherichia coli*.** *Mol Microbiol* 2010, **76**(6):1555–1571.
40. Bremer H, Dennis P: **Modulation of chemical composition and other parameters of the cell by growth rate.** In *Escherichia coli and Salmonella typhimurium: Cellular and Molecular Biology*. Edited by Neidhardt F, Washington, DC: American Society for Microbiology 1996:1553–1569.
41. Klumpp S, Hwa T: **Growth-rate-dependent partitioning of RNA polymerases in bacteria.** *PNAS* 2008, **105**:20245–20250.
42. Bintu L, Buchler N, Garcia H, Gerland U, Hwa T, Kondev J, Phillips R: **Transcriptional regulation by the numbers: models.** *Current Opinion in Genetics and Development* 2005, **15**:116–124.
43. Shea MA, Ackers GK: **The OR control system of bacteriophage lambda, a physical-chemical model for gene regulation.** *Journal of Molecular Biology* 1985, **181**:211–230.
44. Ackers GK, Johnson AD, Shea MA: **Quantative model for gene regulation by λ phage repressor.** *PNAS* 1982, **79**:1129–1133.
45. Camara JE, Breier AM, Brendler T, Austin S, Cozzarelli NR, Crooke E: **Hda inactivation of DnaA is the predominant mechanism preventing hyperinitiation of *Escherichia coli* DNA replication .** *EMBO Reports* 2005, **6**:736–741.
46. von Hippel PH, Berg OG: **On the specificity of DNA-protein interactions.** *Proc Natl Acad Sci U S A* 1986, **83**(6):1608–1612.
47. Godin M, Delgado FF, Son S, Grover WH, Bryan AK, Tzur A, Jorgensen P, Payer K, Grossman AD, Kirschner MW, Manalis SR: **Using buoyant mass to measure the growth of single cells.** *Nat Methods* 2010, **7**(5):387–390.
48. Scott M, Hwa T: **Bacterial growth laws and their applications.** *Curr Opin Biotechnol* 2011.
49. Scott M, Gunderson CW, Mateescu EM, Zhang Z, Hwa T: **Interdependence of cell growth and gene expression: origins and consequences.** *Science* 2010, **330**(6007):1099–1102.
50. Morigen, Molina F, Skarstad K: **Deletion of the *datA* site does not affect once-per-cell-cycle timing but induces rifampin-resistant replication.** *J Bacteriol* 2005, **187**(12):3913–3920.
51. Roth A, Messer W: **High-affinity binding sites for the initiator protein DnaA on the chromosome of *Escherichia coli*.** *Mol Microbiol* 1998, **28**(2):395–401.
52. Fujimitsu K, Senriuchi T, Katayama T: **Specific genomic sequences of *E. coli* promote replicational initiation by directly reactivating ADP-DnaA.** *Genes Dev* 2009, **23**(10):1221–1233.
53. Alon U: *An Introduction to Systems Biology: Design Principles of Biological Circuits*. Chapman & Hall/CRC 2006.
54. Zaslaver A, Kaplan S, Bren A, Jinich A, Mayo A, Dekel E, Alon U, Itzkovitz S: **Invariant distribution of promoter activities in *Escherichia coli*.** *PLoS Comput Biol* 2009, **5**(10):e1000545.
55. Schaechter M, Maaloe O, Kjeldgaard NO: **Dependency on medium and temperature of cell size and chemical composition during balanced growth of *Salmonella typhimurium*.** *Journal of General Microbiology* 1958, **19**(3):592–606.
56. Klumpp S, Zhang Z, Hwa T: **Growth rate-dependent global effects on gene expression in bacteria.** *Cell* 2009, **139**(7):1366–1375.
57. Katayama T, Ozaki S, Keyamura K, Fujimitsu K: **Regulation of the replication cycle: conserved and diverse regulatory systems for DnaA and *oriC*.** *Nat Rev Microbiol* 2010, **8**(3):163–170.
58. Wang X, Lesterlin C, Reyes-Lamothe R, Ball G, Sherratt DJ: **Replication and segregation of an *Escherichia coli* chromosome with two replication origins.** *Proc Natl Acad Sci U S A* 2011, **108**(26):E243–E250.
59. Charbon G, Riber L, Cohen M, Skovgaard O, Fujimitsu K, Katayama T, Løbner-Olesen A: **Suppressors of DnaA(ATP) imposed overinitiation in *Escherichia coli*.** *Mol Microbiol* 2011, **79**(4):914–928.
60. Buchler NE, Louis M: **Molecular titration and ultrasensitivity in regulatory networks.** *J Mol Biol* 2008, **384**(5):1106–1119.

61. Løbner-Olesen A: **Distribution of minichromosomes in individual Escherichia coli cells: implications for replication control.** *EMBO J* 1999, **18**(6):1712–1721.
62. Travers AA: **DNA conformation and protein binding.** *Annual Reviews of Biochemistry* 1989, **58**:427–452.
63. Wang JC, Lynch AS: **Transcription and DNA supercoiling.** *Current Opinion in Genetics and Development* 1993, **3**:764–768.
64. Balke VL, Gralla JD: **Changes in the linking number of supercoiled DNA accompany growth transitions in Escherichia coli.** *J. Bacteriol.* 1987, **169**(10):4499–4506.
65. Flåtten I, Morigen, Skarstad K: **DnaA protein interacts with RNA polymerase and partially protects it from the effect of rifampicin.** *Molecular microbiology* 2009, **71**(4):1018–30.
66. Travers A, Muskhelishvili G: **DNA supercoiling - a global transcriptional regulator for enterobacterial growth?** *Nat Rev Microbiol* 2005, **3**(2):157–169.
67. Gorbatyuk B, Marczynski GT: **Regulated degradation of chromosome replication proteins DnaA and CtrA in Caulobacter crescentus.** *Mol Microbiol* 2005, **55**(4):1233–1245.
68. Collier J, Shapiro L: **Feedback control of DnaA-mediated replication initiation by replisome-associated HdaA protein in Caulobacter.** *J Bacteriol* 2009, **191**(18):5706–5716.
69. Madiraju MVVS, Moomey M, Neuenschwander PF, Muniruzzaman S, Yamamoto K, Grimwade JE, Rajagopalan M: **The intrinsic ATPase activity of Mycobacterium tuberculosis DnaA promotes rapid oligomerization of DnaA on oriC.** *Mol Microbiol* 2006, **59**(6):1876–1890.
70. Klumpp S, Hwa T: **Stochasticity and traffic jams in the transcription of ribosomal RNA: Intriguing role of termination and antitermination.** *PNAS* 2008, **105**:18159–18164.
71. Oeschger MP, Berlyn MKB, Mar N: **Regulation of RNA polymerase synthesis in Escherichia coli: A mutant unable to synthesize the enzyme at 43 degrees.** *Sciences-New York* 1974, **72**(3):911–915.
72. Speck C, Weigel C, Messer W: **ATP- and ADP-DnaA protein, a molecular switch in gene regulation.** *The EMBO Journal* 1999, **18**:6169–6176.

Figures

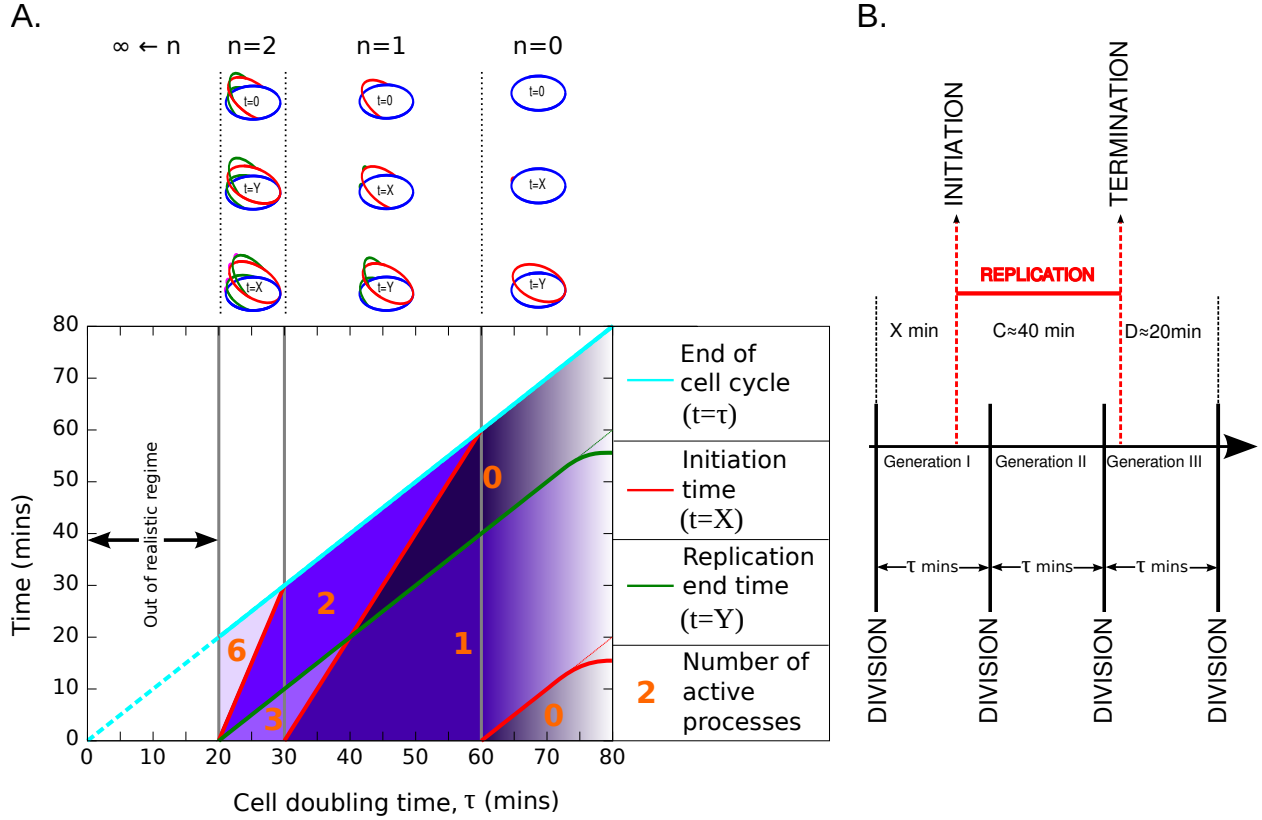
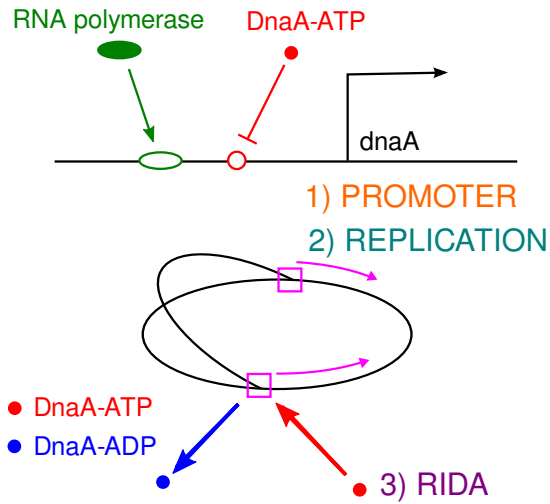


Figure 1: **Timing of DNA replication initiation as a function of the length of the cell cycle according to the Cooper and Helmstetter model.** A: Plots of the values of X , Y and number of active processes (termed \mathcal{F} in the main text) in each region of the graph, for different values of the cell doubling time. The purple shading reflects the number of active processes in each region, with lighter shades denoting a greater number of active processes. Towards $\tau = 80$ mins, the lines $t = X$ and $t = Y$ are shown curving off, showing that this is outside the regime $20 \text{ mins} \leq \tau \leq 60 \text{ mins}$ where the C and D periods can be considered constant. Above the graph in panel A are diagrams of the state of the chromosome for critical time values, for each of the values of n (the number of overlapping replication rounds). B: Illustration of overlapping replication rounds, in the case of a complete replication round of $n = 2$ overlapping rounds, and 3 generations.

A. Ingredients of the model



B. Main Equations

$$\frac{\partial A_-}{\partial t} = \frac{\Theta k_A}{1 + c_1 \frac{\Lambda}{P} + c_2 \frac{A_-}{P}} - k_R F$$

$$\frac{\partial \Lambda}{\partial t} = k_\Lambda F$$

$$\frac{\partial A_+}{\partial t} = k_R F$$

Figure 2: **Ingredients of the model.** A: illustration of 1) the autorepression of the *dnaA* gene 2) the growth of the chromosome by the DNA replication process 3) RIDA taking place at the replication forks. B: The key equations of the model, with the terms colour coded to match the ingredients shown in panel A. The parameters in the model are: A_- (number of DnaA-ATP molecules), A_+ (number of DnaA-ADP molecules), Λ (total genome length), P (number of RNA polymerase molecules), Θ (number of *dnaA* genes), k_A (basal transcription rate of one *dnaA* gene), c_1 , c_2 (binding constants), F (number of pairs of replication forks), k_R (RIDA rate per replication fork), k_Λ (growth rate of the chromosome per replication fork). The first equation represents the change in the number of DnaA-ATP molecules, with a source term due to the *dnaA* promoter (as all newly synthesised DnaA is assumed to bind to ATP due to the relative abundance of ATP in the cell), and a sink term due to the conversion of DnaA-ATP to DnaA-ADP in RIDA. The second equation represents the growth of the genome in the cell. The third equation represents the change in the number of DnaA-ADP molecules. The only source term is the same as the sink term in the DnaA-ATP equation since it is assumed DnaA-ADP is only created from DnaA-ATP during RIDA.

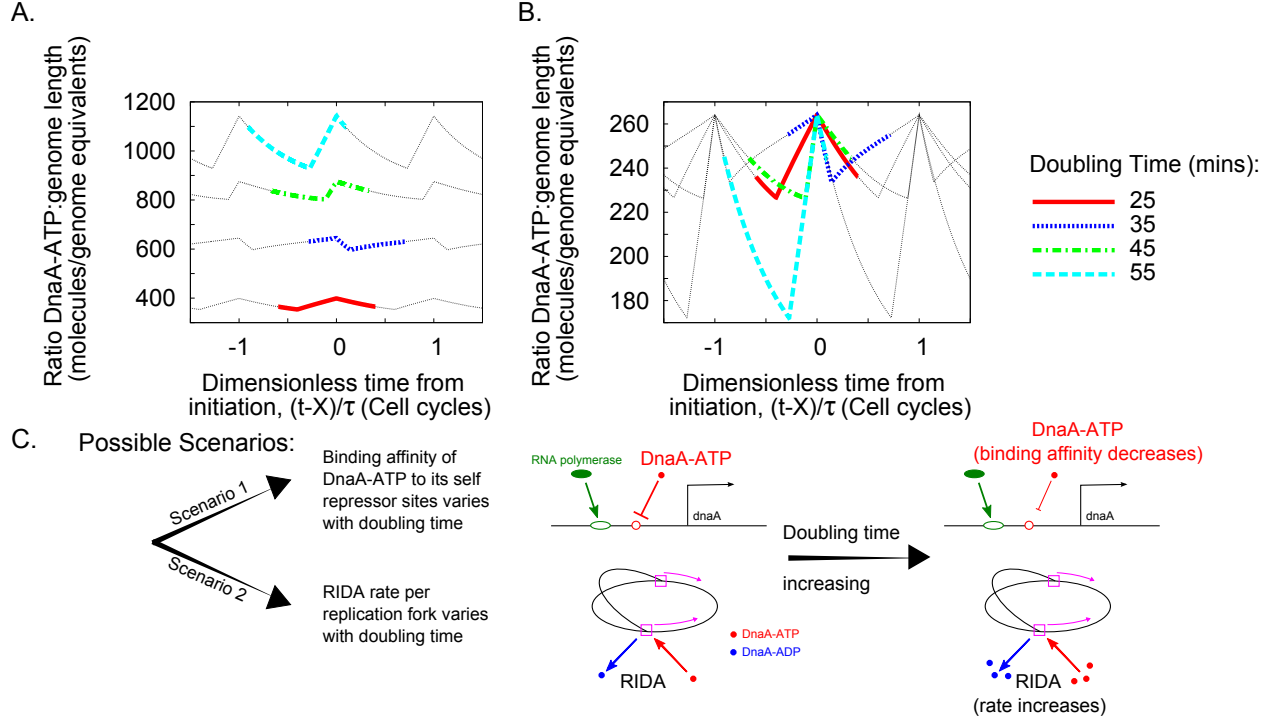


Figure 3: The model imposes a specific DnaA-ATP threshold at the moment of initiation ($t = X$). A: The model with fixed parameters cannot explain an ‘initiation threshold’ since a different value of the ratio DnaA-ATP:genome length (r) is obtained at initiation ($t = X$) for each value of the cell doubling time, τ . B: We perform a mathematical transformation upon the model to impose a threshold for the ratio DnaA-ATP:genome length (r) at the moment of initiation ($t = X$) (in this specific example the threshold has been imposed by allowing the binding affinity of DnaA-ATP to its self repressor site to vary). In both panels A and B, the x -axis has been translated and normalized to denote fractions of cell cycles with the initiation time given by $\frac{t-X}{\tau} = 0$. C: In the case in which both autorepression and RIDA are included in the model there are two scenarios in which an ‘initiation threshold’ can be imposed upon the model. The first of these requires the binding affinity of DnaA-ATP to its self repressor sites to decrease with increasing cell doubling time. The second scenario requires that the RIDA rate increases with increasing cell doubling time. In all scenarios the value of k_A increases with increasing growth rate.

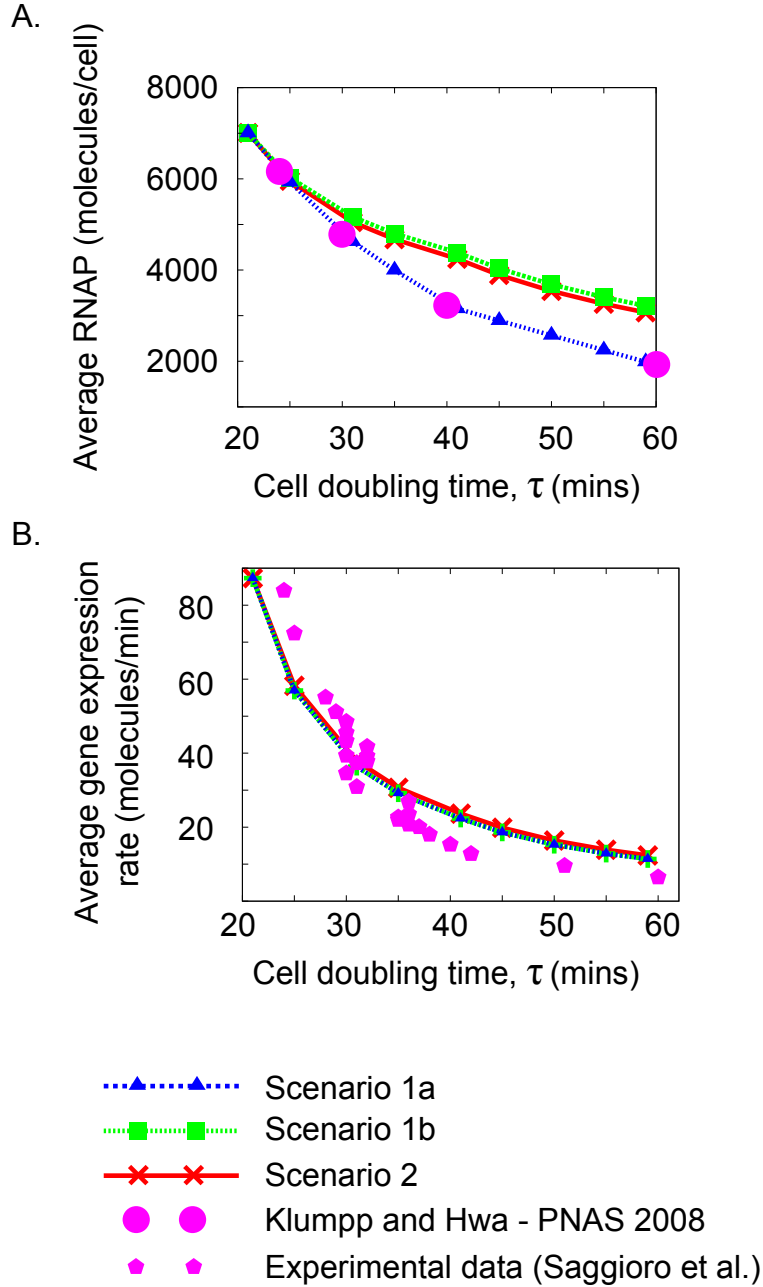


Figure 4: **All scenarios of the model are compatible with previous measurements and predictions.** A: Variation in the average number of RNAP molecules per cell with doubling time. Simulations from the three scenarios (connected triangles, squares and crosses) are compared to the (validated) predictions of ref. [41]. Scenarios 1b and 2 are compatible with the results (which are assumed in scenario 1a). B: Variation in the average expression rate per cell of the *dnaA* gene with growth rate in the three scenarios (connected triangles, squares and crosses) agrees with our direct measurements (Chiara Saggiaro, Anne Olliver, Bianca Sclavi: Multiple levels of regulation in the growth rate dependence of DnaA expression, submitted). The measurements (pentagons) are obtained with GFP reporters on a plasmid, normalized by plasmid number and gene copy-number with varying growth rate. The experiment details are available in Additional File 1, Section 7. This prediction is also compatible with the results of Chiamarello and Zyskind [20].

Consequences of the Scenarios:

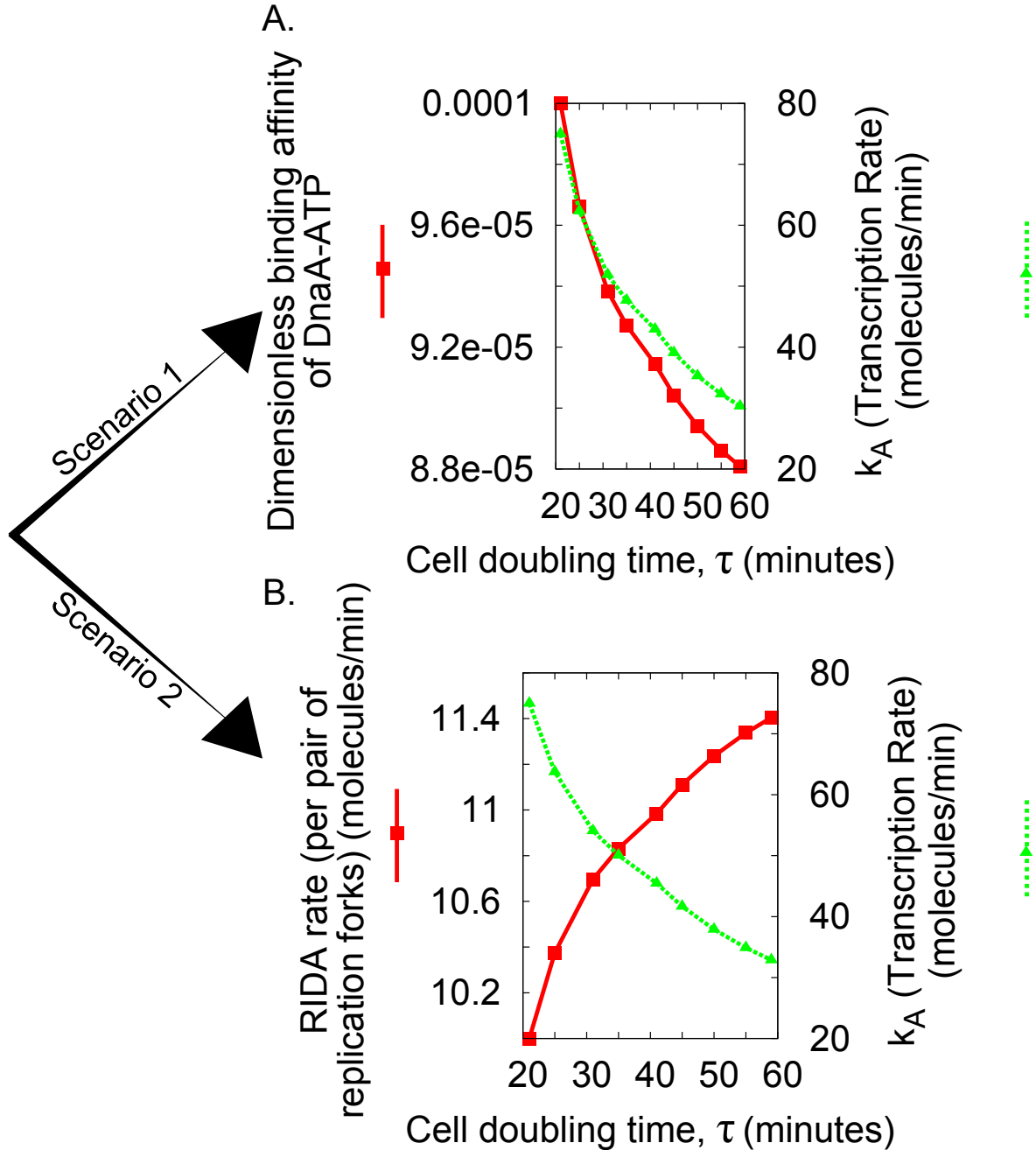


Figure 5: **Predictions of the model can distinguish between different scenarios.** Two possible scenarios can result in a constant initiation threshold for the model. In the first the binding affinity of DnaA-ATP to its repressor sites decreases with increasing cell doubling time, and in the second the RIDA rate increases with cell doubling time. In both scenarios k_A (the basal transcription rate) must decrease with increasing cell doubling time.

Tables

Table 1: **Initial values for the parameters in the model.**

Parameter	Untransformed Value (at $\tau = 21$ mins)	Units	Reference
Basal transcription rate k_A	75	molecules/min	[70]
RNAP binding $e^{\Delta\epsilon_{pd}/k_B T}$	12/10000	Dimensionless	[42]
Dna-ATP binding $e^{\Delta\epsilon_{ad}/k_B T}$	1/10000	Dimensionless	[18], †
RNAP amount P_0	5050	molecules	[41]
RIDA rate k_R	10	molecules/min	[24]
Replication rate k_Λ	1/40	genome equivalents/min	[8]
non-specific binding sites N_{NS}	5×10^6	(genome equivalent) $^{-1}$	[42]

The parameters are fixed with the values in the table for $\tau = 21$ mins and then are able to vary for the other values of τ in order to fix the ratio of DnaA-ATP:chromosome length at the moment of initiation ($t = X$). †: Chiara Saggiaro, Anne Olliver, Bianca Sclavi: Multiple levels of regulation in the growth rate dependence of DnaA expression, submitted.

Table 2: **The dependence of the parameters in the different scenarios.**

Scenario	Floating Parameters	Fixed parameters
1a	k_A, c_1, c_2	P, k_R
1b	k_A, c_2, P	c_1, k_R
2	k_R, k_A, P	c_2, c_1

In all the scenarios, k_A varies with growth rate. In scenario 1a, P changes as a function of growth rate with the values obtained from ref. [41]. The dependence of the other parameters on growth rate is scenario specific (see Additional File 1, Figure A1).

Additional Files

Additional file 1 — Additional Text and Figures

Single pdf file containing the additional text and figures mentioned in the main text.

Additional Text and Figures

Section 1 Considerations on the initiation mass

The initiation mass of *E. coli*, a concept put forward by Donachie in 1968 [10], is an idea that, while independent of the work presented in this paper, has been at the centre of the research into initiation of chromosome replication since its inception. This section presents some thoughts on the implications of our model on the initiation mass argument. As explained in the main text, steady exponential growth of the cell mass is assumed. The volume of the cell at a time t , denoted $\Omega(t)$, is thus

$$\Omega(t) = \Omega_0 e^{\alpha t}, \quad (12)$$

where α is the growth rate such that

$$\alpha = \frac{\log(2)}{\tau} \quad (13)$$

If it is assumed that the initial mass of the cell is an exponential function of the growth rate [55], it is possible, for example, to write

$$\Omega_0 = \Omega_0(\alpha) = \frac{e^{\alpha(C+D)} \Omega_*}{2}, \quad (14)$$

where Ω_* is a constant.

With (12) and (13), this implies that

$$\frac{\Omega(X)}{2^n} = \text{constant} = \Omega_*, \quad (15)$$

where 2^n is the number of *oriC* in the cell. This gives a constant ratio of *oriC* to mass at initiation and so is in agreement with what was shown by Donachie [10].

Donachie's observations of a constant initiation mass are based on the observation by Schaechter et al. [55] of the initial mass of a cell growing exponentially with growth rate. As discussed, for the ratio of the mass to number of origins to be constant at initiation, a very specific initial cell mass is required, namely

$$\Omega(0) = \frac{\Omega_*}{2} e^{\alpha(C+D)}, \quad (16)$$

if the Cooper-Helmstetter model is assumed. However, this particular trend of initial mass with growth rate is not claimed to hold by Schaechter and coworkers: it is simply an exponential relationship that is claimed to hold. Thus, if the relationship was slightly different, say, for example, $\Omega(0) = \frac{\Omega_*}{2} e^{\alpha(C+D+1)}$ then one would have

$$\frac{\Omega(X)}{2^n} = \Omega_* e^\alpha, \quad (17)$$

i.e. the initiation mass would also be an exponential function of the growth rate. So, under the assumption of an initial cell mass varying exponentially with growth rate, it is not necessary to have an initiation mass that is constant; an initiation mass that is a continuous function of growth rate is possible. This study is concerned with determining whether DnaA can fulfill a threshold condition at $t = X$; this question is independent of whether the origin to mass ratio is constant or not at $t = X$.

Section 2 Thermodynamic model for the promoter

This study describes promoter activity using the thermodynamic model first introduced by Shea and Ackers [43,44].

This section introduces the mathematics of the derivation of this term. Note that the term derived here is for the simple autorepressor, which is the form used in the equation (11).

The Shea-Ackers model calculates the probability (assuming equilibrium binding) that RNAP is bound to a given promoter [42]. The validity of the equilibrium binding assumption relies on the rate of binding and unbinding of RNAP to and from the promoter being much faster than the rate of open complex formation. The same is true for the relevant transcription factors (such as DnaA-ATP in this case). Under these assumptions, the probability that RNAP is bound to a particular promoter (in the absence of transcription factors) is given by the ratio of the statistical weight of the state in which RNAP is bound to that promoter, divided by the sum of the statistical weights of all possible states. To formalize this, the number of non-specific binding sites on the chromosome is denoted as N_{NS} and the number of RNAP molecules as P . The number of ways of arranging all the RNAP molecules in the non-specific sites is:

$$\frac{N_{NS}!}{P!(N_{NS} - P)!}, \quad (18)$$

and the statistical weight of this state is thus

$$Z(P) = \underbrace{\frac{N_{NS}!}{P!(N_{NS} - P)!}}_{\text{number of arrangements}} \times \underbrace{e^{-P\varepsilon_{pd}^{NS}/k_B T}}_{\text{Boltzmann weight (binding energy)}}. \quad (19)$$

And so, the probability of having RNAP bound to a given promoter is given by

$$\mathbb{P}(\text{RNAP bound}) = \frac{Z(P-1)e^{-\varepsilon_{pd}^S/k_B T}}{Z_{tot}(P)}, \quad (20)$$

where $Z_{tot}(P)$ represents the sum of the possible statistical weights, namely

$$Z_{tot}(P) = \underbrace{Z(P)}_{\text{promoter unoccupied}} + \underbrace{Z(P-1)e^{-\varepsilon_{pd}^S/k_B T}}_{\text{RNAP bound to promoter}}. \quad (21)$$

What can be seen is that this form of the derivation for the probability of the RNAP being bound to a given promoter does not require the volume to be considered explicitly. The spatial distribution of RNAP within the cell is not considered as it is assumed to provide only a weak perturbation to the probability, given the large number of RNAP molecules in the cell [42].

Now consider the probability for the promoter in the both more relevant and complex case where a repressing transcription factor is involved (namely DnaA-ATP).

The notation used is as follows: Q is the promoter term; A is the number of DnaA-ATP molecules as (where the subscript used in the main text has been dropped for ease of notation); N_{NS} is the number of non-specific binding sites on the chromosome; P is the number of RNAP molecules.

The number of ways of arranging the RNAP molecules and the DnaA-ATP molecules in the non-specific binding sites is

$$\frac{N_{NS}!}{P!A!(N_{NS} - P - A)!} \quad (22)$$

which is effectively the number of arrangements where the appropriate promoter is unoccupied. The statistical weight for this can be written

$$Z(P, A) = \underbrace{\frac{N_{NS}!}{P!A!(N_{NS} - P - A)!}}_{\text{Number of arrangements}} \times \underbrace{e^{-P\varepsilon_{pd}^{NS}/k_B T}}_{\text{weight of each RNAP state}} \times \underbrace{e^{-A\varepsilon_{ad}^{NS}/k_B T}}_{\text{weight of each DnaA-ATP state}}, \quad (23)$$

where the exponential terms are the Boltzmann weights.

Thus, under the assumption that DnaA-ATP acts as an autorepressor, the total statistical weight of all the scenarios is given by

$$\begin{aligned}
Z_{tot}(P, A) = & \underbrace{Z(P, A)}_{\text{empty sites}} \\
& + \underbrace{Z(P-1, A)e^{-\varepsilon_{pd}^S/k_B T}}_{\text{RNAP on promoter}} \\
& + \underbrace{Z(P, A-1)e^{-\varepsilon_{ad}^S/k_B T}}_{\text{DnaA-ATP on specific site}}.
\end{aligned} \tag{24}$$

The probability that RNAP is bound at the *dnaA* promoter is

$$\begin{aligned}
\mathbb{P}(\text{RNAP bound}) &= \frac{Z(P-1, A)e^{-\varepsilon_{pd}^S/k_B T}}{Z_{tot}(P, A)} \\
&= \frac{1}{1 + \frac{N_{NS}}{P}e^{\Delta\varepsilon_{pd}/k_B T} + \frac{A}{P}e^{(\Delta\varepsilon_{pd} - \Delta\varepsilon_{ad})/k_B T}},
\end{aligned} \tag{25}$$

where it has been assumed that $N_{NS} \gg P$ and A .

The basal rate of transcription of the *dnaA* promoter is then defined as k_A and the copy-number of *dnaA* promoters in a given cell at one time (which can be computed from the Cooper-Helmstetter model) as $\Theta(t, \tau)$.

The same kind of argument can be used in order to justify the fact that one expects a constant initiation threshold for DnaA. Consider the fact that 20 DnaA molecules must bind to the origin for initiation to occur. It can be assumed that this state is binary, i.e. that either 20 molecules are bound, or 20 molecules are not bound. The probability of having 20 molecules bound is thus:

$$\mathbb{P}(\text{Origin Bound}) = \frac{Z(A-20)e^{-20\varepsilon_{ao}/k_B T}\omega}{Z(A-20)e^{-20\varepsilon_{ao}/k_B T}\omega + Z(A)},$$

where

$$Z(A) = \frac{N_{NS}!}{A!(N_{NS} - A)!}.$$

Dividing through, and under the assumptions above, gives that

$$\mathbb{P}(\text{Origin Bound}) = \frac{1}{1 + \frac{e^{20\Delta\varepsilon_{ao}/k_B T}}{\omega(\kappa\tau)^{20}}}. \tag{26}$$

Thus, there is a value of r , determined by $\frac{e^{20\Delta\varepsilon_{ao}/k_B T}}{\omega\kappa^{20}}$ at which the probability rapidly approaches unity. This can be seen as the value of r where initiation takes place. Note that this estimate is rather robust to the addition of other possible states, such as states in which DnaA-ATP can be bound to other sites, assuming that the number of these extra specific sites is small in comparison to the total pool of DnaA-ATP molecules.

Section 2.1 Considerations on the increase in RNAP levels

A further factor to consider is the way in which RNAP levels vary during the cell cycle. As with other elements of the cell, the number of RNAP molecules must double during each cell cycle when the bacteria are in exponential growth. The assumption made here is that the RNAP levels grow exponentially during the cell cycle, to reach double their initial value at the end of the cell cycle. Combined with the assumption that the volume of the cells grows exponentially, this means that the concentration of RNAP stays constant through the cell cycle, in agreement with the results of Oeschger et al. [71]. Moreover, even if the levels of RNAP grow linearly, this is only a weak perturbation from the exponential growth. Consequently, the expectation is that this will not significantly affect the model dynamics.

Section 3 Parameter transformation enforcing a constant threshold

This section discusses the parameter transformation of equation (11), providing the key to probing how the parameters of the model must vary with growth rate. As discussed in the main text, equation (11) is transformed to fix the value of r at the moment of initiation ($t = X$) to be the same for every value of τ in the range $20 < \tau < 60$. This is enforced by a translation and scaling on r such that

$$r'(X, \tau) = \lambda(\tau)r(X, \tau) - a(\tau) , \quad (27)$$

where r' is the translated version of r .

The wish is to see what must happen to the coefficients in the equation for the fixed threshold condition to hold, when the structure of (11) is preserved in the transformation. The same transformation can be applied in numerical simulations, but its analytical form is more instructive with respect to classifying the possible parameter transformations.

Equation (11) can be rewritten in the desired form, with translated variables, as

$$\frac{\partial r'}{\partial t} = \frac{1}{\Lambda} \left(\frac{\Theta k'_A}{1 + c'_1 \frac{\Lambda}{P'} + c'_2 \frac{\Lambda}{P'} r'} - (k'_R + r' k_\Lambda) \mathcal{F} \right) . \quad (28)$$

Note that k_Λ cannot change, as this rate is externally imposed by the Cooper-Helmstetter model.

The substitution of r from (27) into equation (11) gives

$$\frac{\partial r'}{\partial t} = \lambda \frac{\partial r}{\partial t} = \frac{\lambda}{\Lambda} \left(\frac{\Theta k_A}{1 + c_1 \frac{\Lambda}{P} + c_2 \frac{\Lambda}{P} \left(\frac{r' + a}{\lambda} \right)} - (k_R + \left(\frac{r' + a}{\lambda} \right) k_\Lambda) \mathcal{F} \right). \quad (29)$$

Comparison of the coefficients of r' and Λ in equation (29) with equation (28), yields the conditions

$$k'_A = \lambda k_A, \quad (30)$$

$$\lambda k_R + a k_\Lambda = k'_R, \quad (31)$$

$$\frac{c_2}{P\lambda} = \frac{c'_2}{P'}, \quad (32)$$

$$\frac{1}{P} \left(c_1 + c_2 \frac{a}{\lambda} \right) = \frac{c'_1}{P'}, \quad (33)$$

and the condition that defines the transformation, namely

$$r'(X) = \lambda r(X) - a = \text{constant}. \quad (34)$$

At this point we note the assumption that the concentration of RNAP is constant throughout the cell cycle. Thus

$$P = P_0 e^{\alpha t} \quad (35)$$

and

$$P' = P'_0 e^{\alpha t} \quad (36)$$

Thus, since equations (32) and (33) have $e^{\alpha t}$ as a common factor, it is possible to divide through by it. From hereafter in this section, P and P' actually refer to P_0 and P'_0 but the subscripts are dropped for ease of notation.

Furthermore, equations (32) and (33) can combine to give

$$a = \frac{c'_1}{c'_2} - \lambda \frac{c_1}{c_2} \quad (37)$$

Examination of equation (4), reveals that

$$\begin{aligned} c_1 &= \frac{b_0}{\kappa} \\ c_2 &= \frac{b_0}{b_1} \end{aligned} \quad (38)$$

where b_0 and b_1 are given by equation (4). Thus, writing $c'_1 = \frac{b'_0}{\kappa}$ and $c'_2 = \frac{b'_0}{b'_1}$ one sees that equation (37) can be rewritten

$$a = \frac{1}{\kappa}(b'_1 - \lambda b_1) \quad (39)$$

where $b_1 = e^{\Delta\varepsilon_{ad}/k_B T}$.

Now, mathematically, two things can be chosen to be fixed to satisfy these equations

1. The RIDA rate can be fixed: $k_R = k'_R$. It then follows from (31) that

$$a = \frac{k_R}{k_\Lambda}(1 - \lambda), \quad (40)$$

which, when combined with equation (39) gives

$$b'_1 = \frac{\kappa k_R}{k_\Lambda}(1 - \lambda) + \lambda b_1. \quad (41)$$

Equation (40), when taken with (34), gives the value that λ must take, namely

$$\lambda = \frac{r'(X) + \frac{k_R}{k_\Lambda}}{r(X) + \frac{k_R}{k_\Lambda}}. \quad (42)$$

Either c_1 (i.e. b_0) or P can then be fixed.

- (a) Since it is possible to choose c'_1 , it is logical to set $c'_1 = c_1$. This gives that, $c'_2 = \frac{b_0}{b'_1}$ and so

$$P' = \frac{b_1 P \lambda}{\left(\kappa \frac{k_R}{k_\Lambda}(1 - \lambda) + \lambda b_1\right)}. \quad (43)$$

Note that any trend for b_0 could have been chosen. The decision to set $b'_0 = b_0$ here, was due to it being the simplest logical choice. This equation, taken with equations (30), (41) and (42) determines the transformation.

- (b) It is possible to fix P' to a known trend e.g. the one given in ref. [41]. This will then have implications for how c_1 (and hence b_0) must vary. Given that P' is now a known quantity, this gives that

$$b'_0 = \frac{b_0 P' \left(\kappa \frac{k_R}{k_\Lambda}(1 - \lambda) + \lambda b_1\right)}{b_1 P \lambda}. \quad (44)$$

This equation, taken with equations (30), (41) and (42) determines the transformation.

2. It is possible to set $c_1 = c'_1$ and $c_2 = c'_2$. From this it follows that

$$a = \frac{c_1}{c_2}(1 - \lambda) \quad (45)$$

and

$$P' = \lambda P. \quad (46)$$

Furthermore,

$$k'_R = \frac{k_R - \frac{c_1}{c_2}(1 - \lambda)k_\lambda}{\lambda}. \quad (47)$$

Thus, equations (45), (46) and (47), along with

$$\lambda = \frac{r'(X) + \frac{c_1}{c_2}}{r(X) + \frac{c_1}{c_2}} \quad (48)$$

and (30), determine the transformation, when c_1 and c_2 are fixed.

Section 4 Average over cell population

This section discusses how to compute average levels of RNA polymerase and average gene expression, used for example in Figure 4. These average levels are quantities that can be in principle measured directly.

Consider, for example, the expression level of the *dnaA* promoter (i.e. Q) (presented in Figure 4B). Denote the average colony expression level as:

$$\text{Average colony expression level} = \langle Q(\alpha) \rangle \quad (49)$$

where steady exponential growth is assumed and α is the growth rate. In order to evaluate this average, the probability of finding a cell at a time $t \in (0, \tau)$ of the cell cycle is required.

Given the exponentially growing colony with growth rate α , let $N(t)$ denote the number of bacteria in the colony at time t . If the interval $(0, \tau)$ is split into $\tau/\delta t$ equal size segments each of infinitesimal size δt , then the number of bacteria born in the infinitesimal time interval $(t, t + \delta t)$ is

$$\delta N(t) = \frac{dN}{dt} \delta t, \quad (50)$$

i.e.

$$\delta N(t) = \alpha N dt = \alpha N_0 e^{\alpha t} \delta t. \quad (51)$$

Within a population of bacteria at time t' , the probability of finding a bacterium born in the time interval $(t_b, t_b + \delta t)$ (with $t_b < t'$) is given by

$$\frac{\delta N(t_b)}{N(t')} = \frac{\alpha N_0 e^{\alpha t_b}}{N(t')} \delta t = \alpha e^{\alpha(t_b - t')} \delta t. \quad (52)$$

This is equivalent to finding a bacterium with an age in the range $(t, t + \delta t)$ where $t = t' - t_b$, and so it can be written that the probability of finding a bacterium with an age in the range $(t, t + \delta t)$ is

$$\mathcal{P}(t, \alpha) = \alpha e^{-\alpha t} \delta t. \quad (53)$$

Moreover, since bacteria divide after a time τ , the probability of finding a bacterium at a stage in the range $(t, t + \delta t)$ of the cell cycle is given by

$$\begin{aligned} \mathbb{P}(t, \alpha) &= \sum_{n=0}^{\infty} \mathcal{P}(n\tau + t) \\ &= \alpha e^{-\alpha t} \sum_{n=0}^{\infty} e^{-\alpha n\tau} \delta t \\ &= \alpha e^{-\alpha t} \left(\frac{1}{1 - e^{-\alpha\tau}} \right) \delta t \\ &= \alpha e^{-\alpha t} \left(\frac{1}{1 - \frac{1}{2}} \right) \delta t \\ &= 2\alpha e^{-\alpha t} \delta t \\ &= \phi(t, \alpha) \delta t \end{aligned} \quad (54)$$

Note that the individual bacteria are assumed to grow exponentially with growth rate α in the same way as the colony itself. Thus,

$$\begin{aligned} \langle Q(\alpha) \rangle &= \sum_{m=0}^{\tau/\delta t} Q(m\delta t, \alpha) \mathbb{P}(m\delta t, \alpha) \\ &= \sum_{m=0}^{\tau/\delta t} Q(m\delta t, \alpha) \phi(m\delta t, \alpha) \delta t \\ &= \int_0^{\tau} Q(t, \alpha) \phi(t, \alpha) dt \end{aligned} \quad \text{in the limit as } \delta t \rightarrow 0 \quad (55)$$

This argument gives the average value of any observable quantity. For example to get the average of P , as in Figure 4A, one would take

$$\langle P(\alpha) \rangle = \int_0^\tau P(t, \alpha) \phi(t, \alpha) dt. \quad (56)$$

Section 5 Considerations on other forms of the promoter

This section deals with thermodynamic models for promoters that incorporate some further experimental findings on the behaviour of the *dnaA* gene [24]. Data from footprint experiments has provided an insight into the cooperativity of the DnaA boxes on the *dnaA* gene, which has been proposed to be important for the correct timing of DNA replication in *Escherichia coli*, as well as potential autoactivation of the gene [72]. The models considered are (i) a promoter with no autorepression, (ii) a model with cooperativity of DnaA binding to the repression sites at the *dnaA* promoter, (iii) a promoter with both cooperativity and autoactivation. The reasons for not choosing these model variants as the main model formulation are then discussed.

Section 5.1 Promoter with no autorepression

This section considers a simpler model for the promoter than the one used in the main text, namely one that has no autorepression. The form for this type of promoter was derived in Section 2 and its implications are discussed more fully here. When the results from Section 2 are used, the main equation takes the form

$$\frac{\partial r}{\partial t} = \frac{1}{\Lambda} \left(\frac{\Theta k_A}{1 + c_1 \frac{\Lambda}{P}} - (k_R + r k_\Lambda) \mathcal{F} \right). \quad (57)$$

This is integrated, with fixed parameters k_A , c_1 , k_R and k_Λ assumed, to give $r(t, \tau)$, for a given τ . The parameter c_1 is then varied (for a fixed value of τ) to probe the effect that autorepression has (see Figure A2). What can be seen in Figure A2 is that autorepression causes the range of values for $r(t, \tau)$ (the oscillation size), to be much narrower than for the non-autorepressed case. This might be an important role that autorepression plays in fine tuning the timing of replication initiation, since it ensures that, even before any other parameters are considered to be variable, the differences in the ratio DnaA-ATP:DNA length is reduced across different τ . For this reason, autorepression was chosen to be included in the main model formulation.

Section 5.2 Promoter with cooperativity of DnaA binding

This section discusses a model for a promoter in which there are two binding sites for DnaA. First, it deals with a form for a simple case of cooperativity, and then it introduces a more complex form including differential action of

DnaA-ATP and DnaA-ADP.

Section 5.2.1 Simple cooperativity

In the model considered here, there are two binding sites for DnaA, both of which have a repression effect when bound, and which bind highly cooperatively. The sites are considered to have a low affinity for DnaA so only a probability to the situation in which both sites are bound is allocated. As in Section 2, the number of DnaA-ATP molecules is denoted as A , the number of non-specific binding sites as N_{NS} and the number of RNA polymerase molecules as P . Furthermore, the binding energy between a molecule x and a (non-)specific site on the DNA is defined as $\varepsilon_{xd}^{(N)S}$ and the difference is denoted as

$$\Delta\varepsilon_{xd} = \varepsilon_{xd}^S - \varepsilon_{xd}^{NS}. \quad (58)$$

In addition, the cooperativity of binding between two DnaA-ATP molecules is written as ω .

Thus, the sum of all the statistical weights is

$$Z_{tot} = \underbrace{Z(P, A)}_{\text{Empty sites}} + \underbrace{Z(P-1, A)e^{-\varepsilon_{pd}^S}}_{\text{RNAP bound}} + \underbrace{Z(P, A-2)e^{-2\varepsilon_{ad}^S\omega}}_{\text{DnaA-ATP bound cooperatively}}. \quad (59)$$

This form allocates zero probability that DnaA-ATP can bind by itself. This leads directly to the probability of RNAP being bound to the promoter, namely

$$\mathbb{P}(\text{RNAP bound}) = \frac{Z(P-1, A)e^{-\varepsilon_{pd}^S}}{Z_{tot}}, \quad (60)$$

i.e.

$$\mathbb{P}(\text{RNAP bound}) = \frac{1}{1 + e^{\Delta\varepsilon_{pd} \frac{N_{NS}}{PF_{reg}}}}, \quad (61)$$

where

$$F_{reg}^{-1} = 1 + e^{-2\Delta\varepsilon_{ad}\omega} \left(\frac{A}{N_{NS}} \right)^2. \quad (62)$$

Figure A6C shows that the presence of cooperativity alone cannot produce a constant threshold. Thus, it is necessary to try and impose a constant threshold on the model using a transformation such as that described in Section 3. Now, if it is written that $r\kappa = \frac{A}{N_{NS}}$ (see main text for definition of κ), an attempt to perform the same transformation as in Section 3, i.e.

$$r' = \lambda r - a, \quad (63)$$

shows that the $(r\kappa)^2$ term produces a linear term in r' that is not present in the original form of F_{reg} and so the transformation will fail as it will not generally be possible to retain the original form of the model.

Section 5.2.2 A more sophisticated model for cooperativity

We consider here the more realistic situation where the two binding sites differ. One is a high-affinity site, which does not contribute towards autorepression, and the other is a low-affinity site to which DnaA binds cooperatively and such that, when bound, DnaA has a repression effect on the *dnaA* gene [18]. The number of ways of distributing P RNA polymerase molecules and A DnaA-ATP molecules in N_{NS} binding sites is thus

$$Z(P, A) = \frac{N_{NS}!}{P!A!(N_{NS} - P - A)} \times e^{-P\varepsilon_{pd}^{NS}} e^{-A\varepsilon_{ad}^{NS}}. \quad (64)$$

There are five different possible states of the system, described in the sum of the statistical weights:

$$\begin{aligned} Z_{tot} = & \underbrace{Z(P, A)}_{\text{Empty sites}} \\ & + \underbrace{Z(P-1, A)e^{-\varepsilon_{pd}^S}}_{\text{RNAP bound}} \\ & + \underbrace{Z(P-1, A-1)e^{-(\varepsilon_{pd}^S + \varepsilon_{ad}^H)}}_{\text{RNAP bound and high affinity site bound}} \\ & + \underbrace{Z(P, A-1)e^{-\varepsilon_{ad}^H}}_{\text{High affinity site bound and RNAP not bound}} \\ & + \underbrace{Z(P, A-2)e^{-(\varepsilon_{ad}^H + \varepsilon_{ad}^L)}\omega}_{\text{DnaA-ATP bound cooperatively}}. \end{aligned} \quad (65)$$

This model allocates zero probability that DnaA-ATP can bind to the low-affinity site alone. For it to bind to this site it must do so cooperatively once the high affinity site is bound.

This leads to the probability of RNAP being bound to the promoter, namely:

$$\mathbb{P}(\text{RNAP bound}) = \frac{Z(P-1, A)e^{-\varepsilon_{pd}^S} + Z(P-1, A-1)e^{-(\varepsilon_{pd}^S + \varepsilon_{ad}^H)}}{Z_{tot}}, \quad (66)$$

i.e.

$$\mathbb{P}(\text{RNAP bound}) = \frac{1}{1 + e^{\Delta\varepsilon_{pd}} \frac{N_{NS}}{PF_{reg}}} \quad (67)$$

where

$$F_{reg}^{-1} = \frac{1 + \frac{A}{N_{NS}} e^{-\Delta\epsilon_{ad}^H} + \omega \left(\frac{A}{N_{NS}} \right)^2 e^{-(\Delta\epsilon_{ad}^H + \Delta\epsilon_{ad}^L)}}{1 + \frac{A}{N_{NS}} e^{-\Delta\epsilon_{ad}^H}}. \quad (68)$$

Now, writing $r\kappa = \frac{A}{N_{NS}}$ (see main text for definition of κ), the same transformation as for the main equation can be performed, following the steps in Section 3, i.e. writing

$$r' = \lambda r - a \quad (69)$$

and collecting and comparing terms in r' .

Section 5.3 Promoter with both cooperativity and autoactivation

This section considers an even more realistic form for the promoter which incorporates both autoactivation and cooperativity of DnaA binding of both forms of bound DnaA. The main conclusion is that this representation introduces too many new parameters in the model, which cannot be estimated from experiments, and therefore adds uncontrolled uncertainty. Hence, priority was given to the simpler and more controlled model presented in the main text.

First, consider the *dnaA* gene itself, which has in fact two promoters, *dnaAp1* and *dnaAp2*. Since the expression of the *dnaA* gene is controlled mostly by the *dnaAp2* promoter, only this promoter is considered. There are 5 DnaA boxes on the *dnaA* gene, two high affinity boxes (1 and 2) which bind both DnaA-ATP and DnaA-ADP and three low affinity boxes (a, b and c) which bind only DnaA-ATP. Since box a appears to only affect the *dnaAp1* promoter, it is ignored for this derivation. DnaA boxes b and c appear to cause autorepression when bound by DnaA-ATP.

Boxes 1 and 2 appear to cause autoactivation when bound by either DnaA-ATP or DnaA-ADP in situations when DnaA boxes b and c are unbound. Moreover, it is assumed that, due to cooperativity, there must be pairwise binding between boxes 1 and 2 and boxes b and c i.e. if box 1 is bound by DnaA-ATP then box 2 must also be bound by DnaA-ATP [72].

In a similar manner to the previous section, the number of DnaA-ATP molecules is denoted as A_- , the number of DnaA-ADP molecules as A_+ , the number of non-specific binding sites as N_{NS} and the number of RNA polymerase molecules as P . Furthermore, the binding energy between a molecule x and a (non-)specific site, i , on the DNA is defined as $\epsilon_{xd}^{(N)S_i}$ and the difference as

$$\Delta\epsilon_{xd} = \epsilon_{xd}^{S_i} - \epsilon_{xd}^{NS}. \quad (70)$$

In addition to this, the binding energy (cooperativity) between two molecules a and b is written as ε_{ab} . So, the statistical weight of distributing P RNA polymerase molecules, A_- DnaA-ATP molecules and A_+ DnaA-ADP molecules among N_{NS} non-specific binding sites is

$$Z(P, A_-, A_+) = \frac{N_{NS}!}{P!A_-!A_+!(N_{NS} - P - A_- - A_+)} \times e^{-P\varepsilon_{Pd}^{NS}} e^{-A_-\varepsilon_{A-d}^{NS}} e^{-A_+\varepsilon_{A+d}^{NS}}. \quad (71)$$

The sum of all the statistical weights is

$$\begin{aligned} Z_{tot} = & Z(P, A_-, A_+) + Z(P-1, A_-, A_+)e^{-\varepsilon_{Pd}^S} \\ & + Z(P, A_- - 2, A_+)k_{b,c} + Z(P-1, A_- - 2, A_+)e^{-\varepsilon_{Pd}^S}k_{1,2}^-\omega_{0,1}^- \\ & + Z(P, A_- - 2, A_+)k_{1,2}^- + Z(P, A_-, A_+ - 2)k_{1,2}^+ \\ & + Z(P, A_- - 4, A_+)k_{b,c}k_{1,2}^-\omega_{b,1}^- + Z(P-1, A_-, A_+ - 2)e^{-\varepsilon_{Pd}^S}k_{1,2}^+\omega_{0,1}^+ \\ & + Z(P, A_- - 2, A_+ - 2)k_{b,c}k_{1,2}^+\omega_{b,1}^+, \end{aligned} \quad (72)$$

where

$$\begin{aligned} k_{b,c} &= e^{-2\varepsilon_{A-d}^{S_{b,c}}} \\ k_{1,2}^- &= e^{-2\varepsilon_{A-d}^{S_{1,2}}} \\ k_{1,2}^+ &= e^{-2\varepsilon_{A+d}^{S_{1,2}}} \\ \omega_{0,1}^- &= e^{-\varepsilon_{A-P}} \\ \omega_{0,1}^+ &= e^{-\varepsilon_{A+P}} \\ \omega_{b,1}^+ &= e^{-\varepsilon_{A-A_+}^{b,1}} \\ \omega_{b,1}^- &= e^{-\varepsilon_{A-A_-}^{b,1}}. \end{aligned} \quad (73)$$

Thus, the probability of RNA polymerase being bound to the *dnaA* promoter is

$$\begin{aligned} \mathbb{P}(\text{RNAP bound}) = & \frac{1}{Z_{tot}} \left(Z(P-1, A_-, A_+)e^{-\varepsilon_{Pd}^S} + Z(P-1, A_- - 2, A_+)e^{-\varepsilon_{Pd}^S}k_{1,2}^-\omega_{0,1}^- \right. \\ & \left. + Z(P-1, A_-, A_+ - 2)e^{-\varepsilon_{Pd}^S}k_{1,2}^+\omega_{0,1}^+ \right), \end{aligned} \quad (74)$$

i.e.

$$\mathbb{P}(\text{RNAP bound}) = \frac{1}{1 + e^{\Delta \varepsilon_{Pd} \frac{N_{NS}}{P F_{reg}}}}, \quad (75)$$

where

$$F_{reg}^{-1} = \frac{1 + \Delta k_{b,c} \left(\frac{A_-}{N_{NS}} \right)^2 + \Delta k_{1,2}^- \left(\frac{A_-}{N_{NS}} \right)^2 + \Delta k_{1,2}^+ \left(\frac{A_+}{N_{NS}} \right)^2 + \Delta k_{b,c} \Delta k_{1,2}^- \omega_{b,1}^- \left(\frac{A_-}{N_{NS}} \right)^4 + \Delta k_{b,c} \Delta k_{1,2}^+ \frac{A_-^2 A_+^2}{N_{NS}^4}}{1 + \Delta k_{1,2}^- \omega_{0,1}^- \left(\frac{A_-}{N_{NS}} \right)^2 + \Delta k_{1,2}^+ \omega_{0,1}^+ \left(\frac{A_+}{N_{NS}} \right)^2}, \quad (76)$$

where it has been assumed that $N_{NS} \gg P$, A_- and A_+ . In this equation, $\Delta k_{i,j}^{(+/-)} = k_{i,j}^{(+/-)} \times e^{2(\varepsilon_{A_+/-}^{NS})}$.

Now, if the substitution $r\kappa = \frac{A_-}{N_{NS}}$ is used (see main text for definition of κ), then when a transformation such as that in Section 3, namely

$$r' = \lambda r - a, \quad (77)$$

is attempted, it can be seen that the $(r\kappa)^2$ and $(r\kappa)^4$ terms will create terms that are linear, and cubic, in r' . Thus, it is not possible in general to make a scaling and translation on r in this way and keep the F_{reg} in the same form. This information shows that this model of the promoter, with fixed parameters, cannot explain a constant threshold for the ratio r at initiation, and suggests that analyzing this promoter poses a different problem altogether as it cannot be done by applying the techniques used in this work for the more simple promoter. Moreover, equation (73) introduces many new parameters in the model, which generally cannot be directly estimated from experiments, and therefore adds an element of uncertainty into the model. For this reason it is believed that, while the promoter model is satisfactory with respect to existing footprinting data [72], in absence of more precise knowledge, a simple controlled model such as the one presented in the main text is to be preferred.

Section 6 Considerations on other model ingredients

Section 6.1 DnaA-ATP recycling regions

As explained in the main text, the DnaA recycling sequences, known to convert the ADP-bound form of DnaA into its ATP-bound form were considered in a model variant. Here we discuss the mathematics of including a term in the equation to represent this reactivation. We show how it counters RIDA, with a rate that is proportional to the genome amount rather than genome replication rate, and analyze its effects under variations of the growth rate.

The number of the DnaA recycling sites is assumed to be proportional to the total length of the genome in the cell.

Furthermore, regeneration is assumed to be replication fork independent, and it is assumed that the rate limiting

parameter is the recycling rate per recycling site, rather than the amount of DNA-ADP in the cell. Thus the new, effective, RIDA term becomes:

$$\tilde{k}_R = k_R - \rho \frac{\Lambda}{\mathcal{F}}, \quad (78)$$

where ρ is the recycling rate per length of chromosome (i.e. ρ is (the recycling rate per site) \times (the number of recycling sites per genome equivalent)). Performing the same transformation as in equation (27) gives

$$k'_R = \lambda k_R + a k_\Lambda \quad (79)$$

and

$$\rho' = \lambda \rho \quad (80)$$

i.e. unless $\lambda = 1$, the recycling rate per site must also vary with growth rate. This indicates that the effect of DARS recycling is not able by itself to impose a constant threshold with varying growth rate.

Note that one now has

$$\tilde{k}'_R = \lambda \tilde{k}_R + a k_\Lambda, \quad (81)$$

which is equivalent to equation (31) with \tilde{k}_R in place of k_R . Thus this new, effective RIDA rate behaves similarly as the previous RIDA rate does in the main equation, scaling and translating as a function of cell doubling time.

Section 6.2 Specific binding sites for DnaA

This section considers a model variant including specific sites along the chromosome, at which DnaA-ATP can bind, providing a titrating effect reducing the reservoir of free DnaA-ATP that can be bound non-specifically on the chromosome. We show that the inclusion of a term of this form is equivalent to a reduction of the RIDA rate.

Let β denote the number of specific binding sites per genome equivalent. We further assume that once these specific binding sites are created, they are (nearly) always bound by a DnaA-ATP molecule. Thus

$$\begin{aligned} \frac{\partial A_-}{\partial t} &= Q - k_R \mathcal{F} - \beta \frac{\partial \Lambda}{\partial t} \\ &= Q - (k_R + \beta k_\Lambda) \mathcal{F}, \end{aligned} \quad (82)$$

where A_- now represents the ‘free’ DnaA-ATP. Thus, equation (82) is the same as the main equation for $\frac{\partial A_-}{\partial t}$, but with an effective increase of the RIDA rate due to titration, where the new, effective, RIDA rate is given by

$$\tilde{k}_R = k_R + \beta k_\Lambda. \quad (83)$$

$\beta \approx 300$ and $k_\Lambda = \frac{1}{40} \text{min}^{-1}$, hence $\beta k_\Lambda \approx 7.5 \text{min}^{-1}$. As shown in Additional Figure A8, the model is robust to changes in the RIDA rate of this order of magnitude, and thus adding the role of specific binding sites does not affect the qualitative behavior of the model.

Section 7 Experimental Methods

Escherichia coli K-12 strains BW25113 carrying the pKK-*gfp* plasmid, where the reporter gene *gfp* (green fluorescent protein) was expressed under control of the *dnaA* promoter region (PdnaA), were grown at 37°C in four different M9 minimal media to support different growth rates. Fluorescence and optical density were measured as a function of time with an automated temperature-controlled plate reader Wallac Victor3. Gene expression was calculated by taking the time derivative of the fluorescence divided by the optical density, which provides a measure of the promoter activity as previously described [54].

To obtain data for the promoter activity as a function of growth rate during exponential phase, an exponential window was automatically detected by taking as maximum value the inflection point of the OD curve and as minimal value the first OD value that is two times higher than the OD background value. In this window the data was then fitted to an exponential function and this fit was used in order to extract the values of generation time. Expression data for different growth rates were corrected for plasmid abundance.

Section 8 Additional Figures

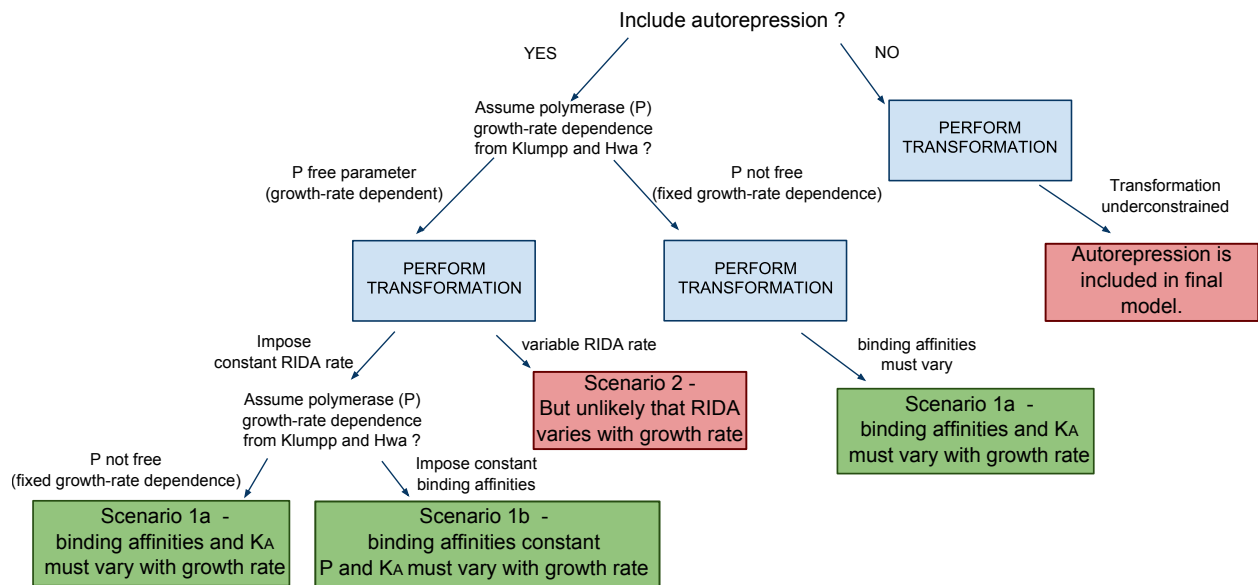


Figure A1: **Flow-chart of the procedure adopted for defining the scenarios of parameter variation with growth rate.**

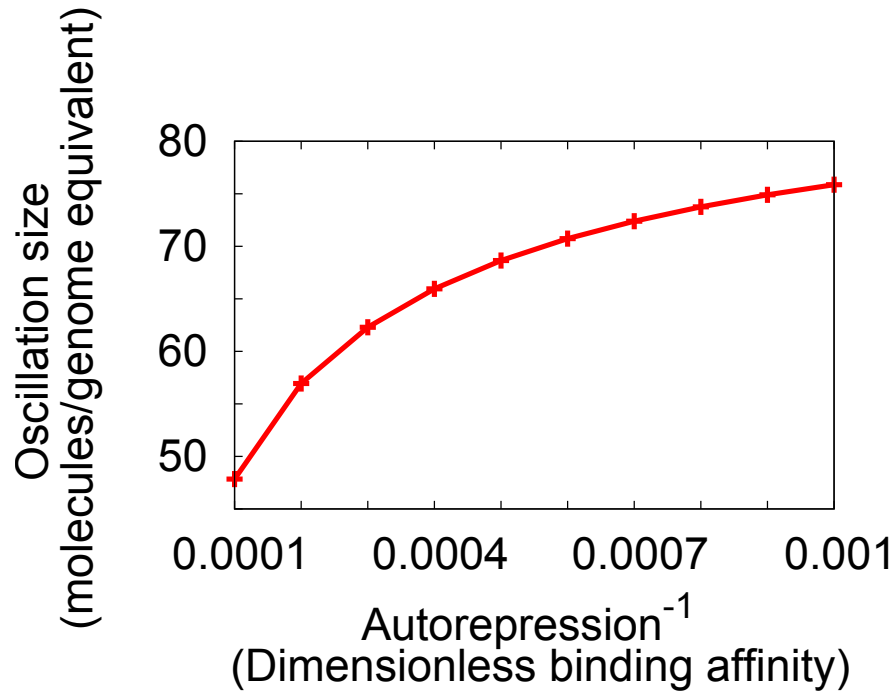


Figure A2: **Autorepression reduces the amplitude of the oscillations of the cell cycle.** If one varies the dimensionless binding affinity of DnaA-ATP to its self-repression sites, one can effectively vary the amount of autorepression. As the amount of autorepression is increased, the amplitude of the oscillations of the cell cycle decrease. The amplitude is defined as the difference between the maximum and minimum values of r in a given cell cycle. This cell cycle length in this plot is $\tau = 35$ mins.

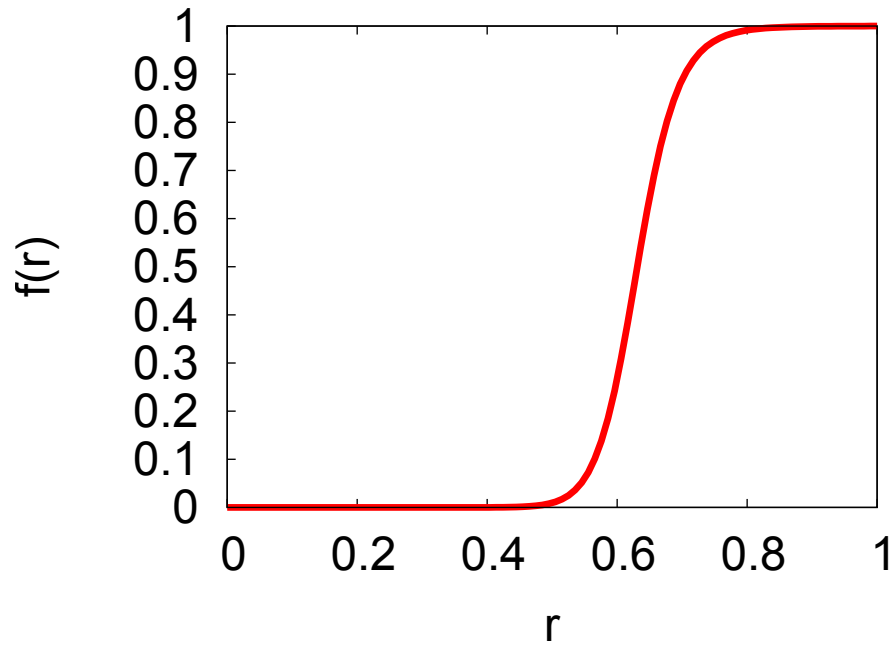


Figure A3: **There is a critical value at which the probability of DnaA-ATP molecules binding to the origin quickly approaches unity.** In this plot, $f(r) = \frac{1}{\omega e^{20\Delta\varepsilon/k_B T} r^{-20} + 1}$, which is the probability of having 20 DnaA-ATP molecules bound to the origin, where we have taken $\omega e^{20\Delta\varepsilon/k_B T} = 0.0001$ in this case.

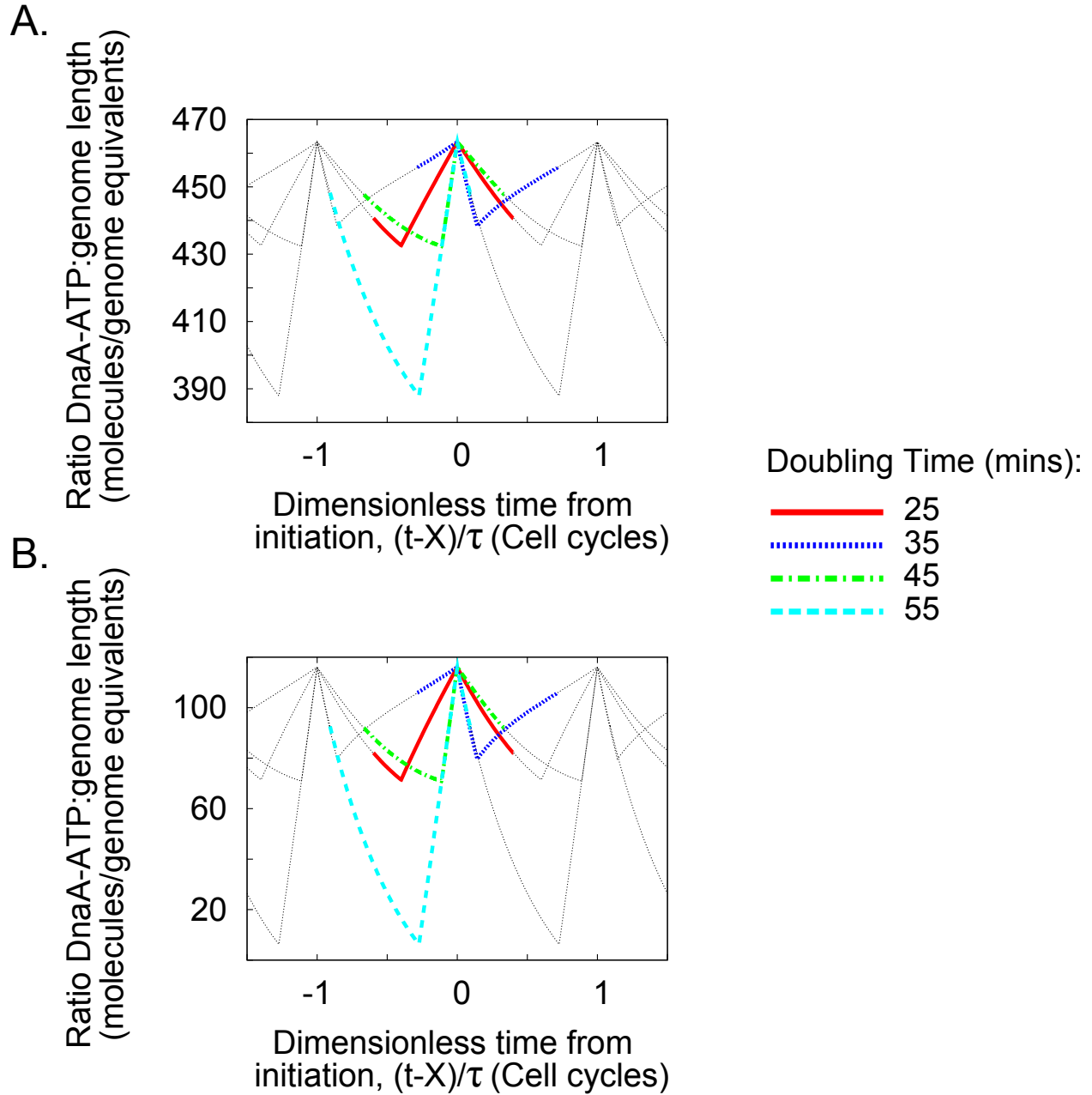


Figure A4: **A constant threshold can still be achieved when the RIDA rate k_R is varied significantly.** A: The oscillations of the cell cycle when $k_R = 2$ molecules/minute. B: The oscillations of the cell cycle when $k_R = 17$ molecules/minute. Despite RIDA rates being nearly 10 fold different, a constant threshold can still be achieved for each.

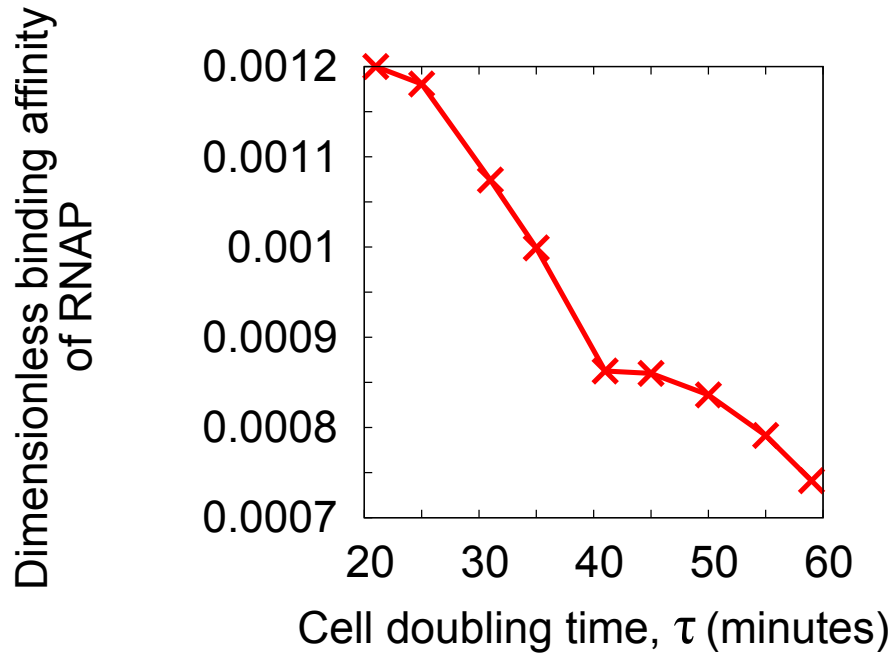


Figure A5: In scenario 1a, the binding affinity of RNAP to the DnaA promoter ($e^{\Delta\varepsilon_{pd}/k_B T}$) varies with cell doubling time (τ). In particular it decreases with cell doubling time, in a similar manner to the binding affinity of DnaA-ATP. This could be caused by supercoiling.

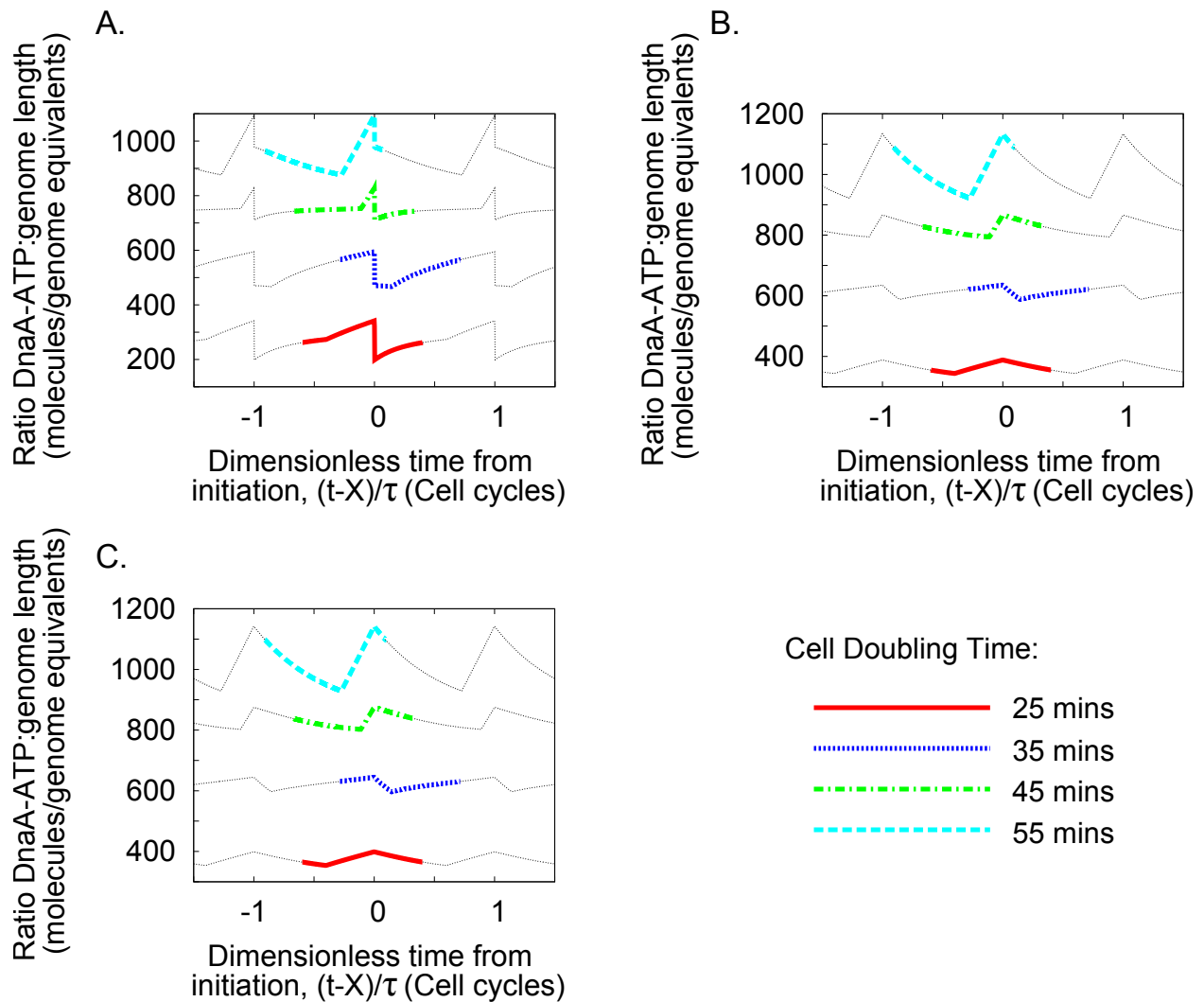


Figure A6: **Model variants were considered which all fail to explain a constant initiation threshold in r .** The models include: A: The *datA* locus, binding up to 300 DnaA-ATP molecules soon after initiation. B: A delay in the synthesis of DnaA-ATP, to reflect the time interval between the mRNA being transcribed and the DnaA protein being translated. C: A more complex form for the *dnaA* promoter, containing two binding sites for DnaA which binds cooperatively. None of these variants succeeds in achieving a constant initiation threshold in r , leading us to pursue a model in which some of the parameters of the model are able to vary with growth rate.

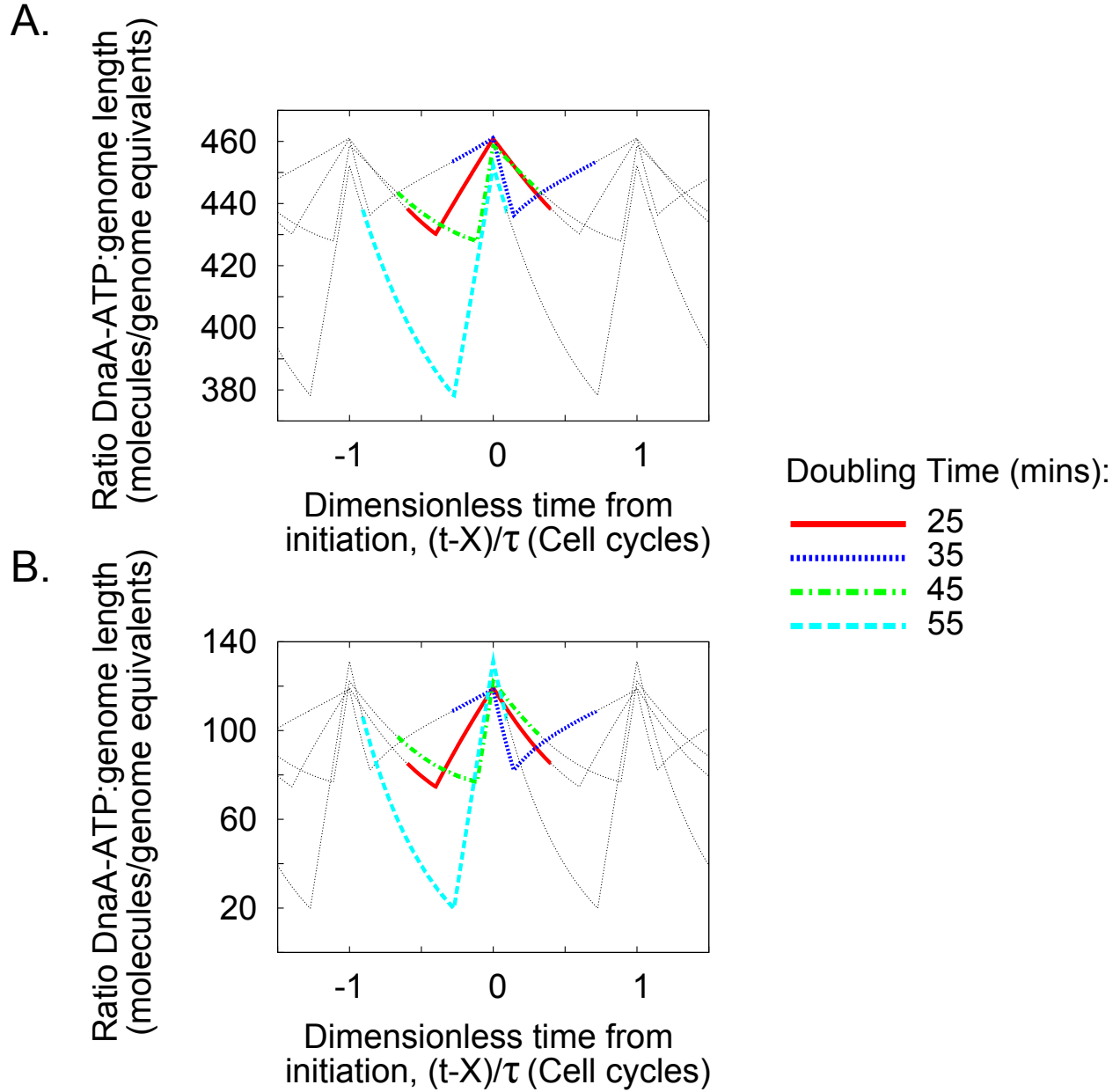


Figure A7: **A mutant in which the RIDA rate is varied.** Attempting to reproduce the effect of over or under-expressing the Hda protein or sequestering DnaA from specific titration sites uniformly distributed along the genome, we modified the RIDA rate leaving the other parameters fixed to their values when $k_R = 10$ molecules/minute. A: The RIDA rate is reduced to $k_R = 2$ molecules/minute, resulting in a lower value of r at $t = X$ at slower growth rates, and thus later initiation time. B: The RIDA rate is increased to $k_R = 17$ molecules/minute, resulting in a higher value of r at $t = X$ at slower growth rates, and thus earlier initiation time.

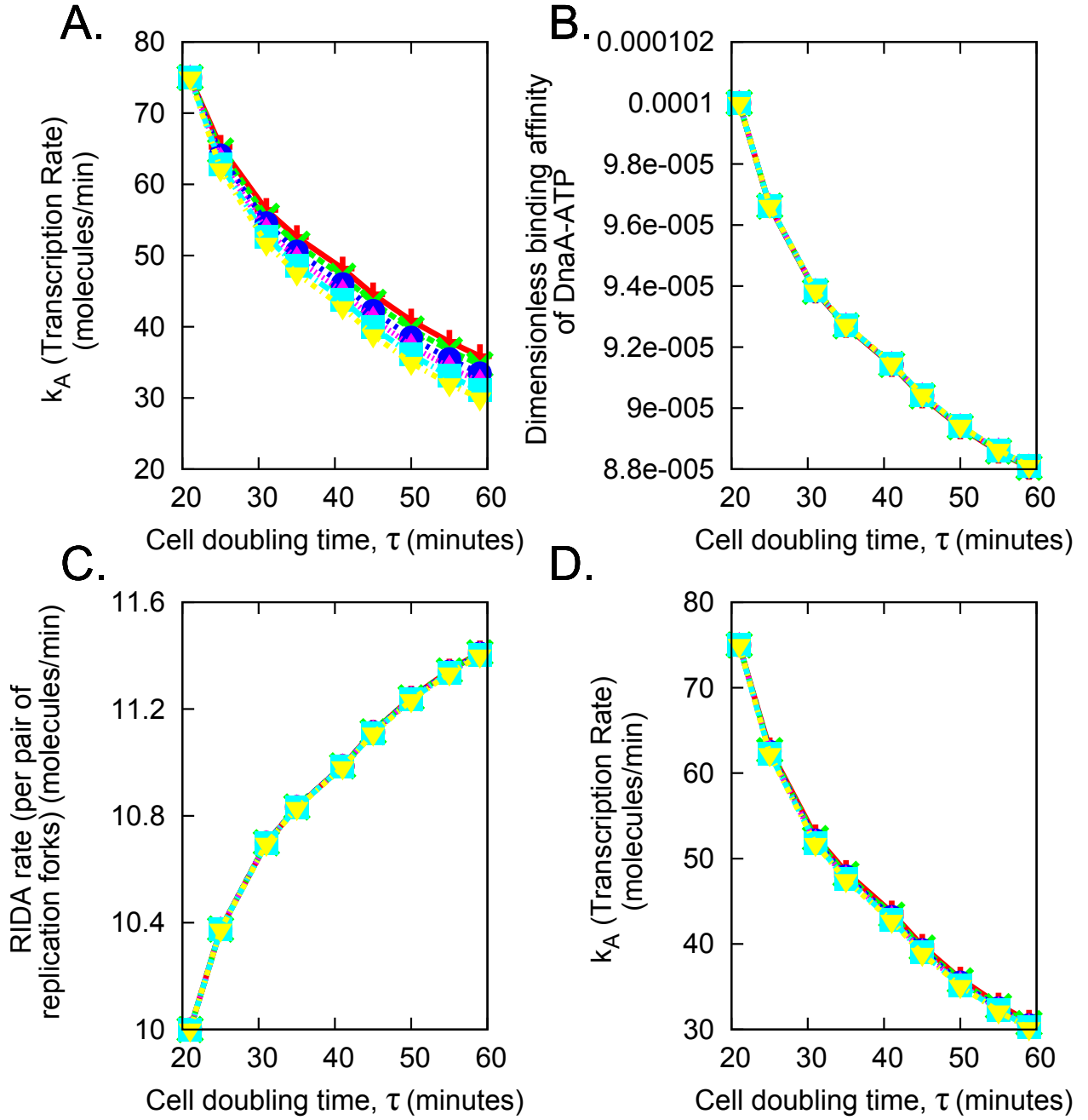


Figure A8: **The model is robust to changes in the input parameters.** In order to show that the qualitative trends, observed from transforming the main equation, were independent of the choice of parameters, the values of the input parameters were varied and the trends replotted. A: The trend of k_A as the value of the RIDA rate, k_R , is varied, with $k_R \in \{5, 7, 9, 11, 13, 15\}$, denoted by the symbols, $+$, \times , \bullet , \blacktriangle , \blacksquare , \blacktriangledown respectively. B: The trend of the dimensionless binding affinity of DnaA-ATP to its self-repression sites as k_A is varied, with $k_A \in \{50, 60, 70, 80, 90, 100\}$, denoted by the symbols, $+$, \times , \bullet , \blacktriangle , \blacksquare , \blacktriangledown respectively. C: The trend of the RIDA rate, k_R as the dimensionless binding affinity of RNAP to the DnaA promoter is varied, with $e^{\Delta\epsilon_{pd}/k_B T} \in 10^{-4} \times \{5, 7, 9, 11, 13, 15\}$, denoted by the symbols, $+$, \times , \bullet , \blacktriangle , \blacksquare , \blacktriangledown respectively. D: The trend of k_A as the dimensionless binding affinity of RNAP to the DnaA promoter is varied, with $e^{\Delta\epsilon_{pd}/k_B T} \in 10^{-4} \times \{5, 7, 9, 11, 13, 15\}$, using the same symbols as in C. In all the plots, the qualitative trend is the same for all the parameter values.

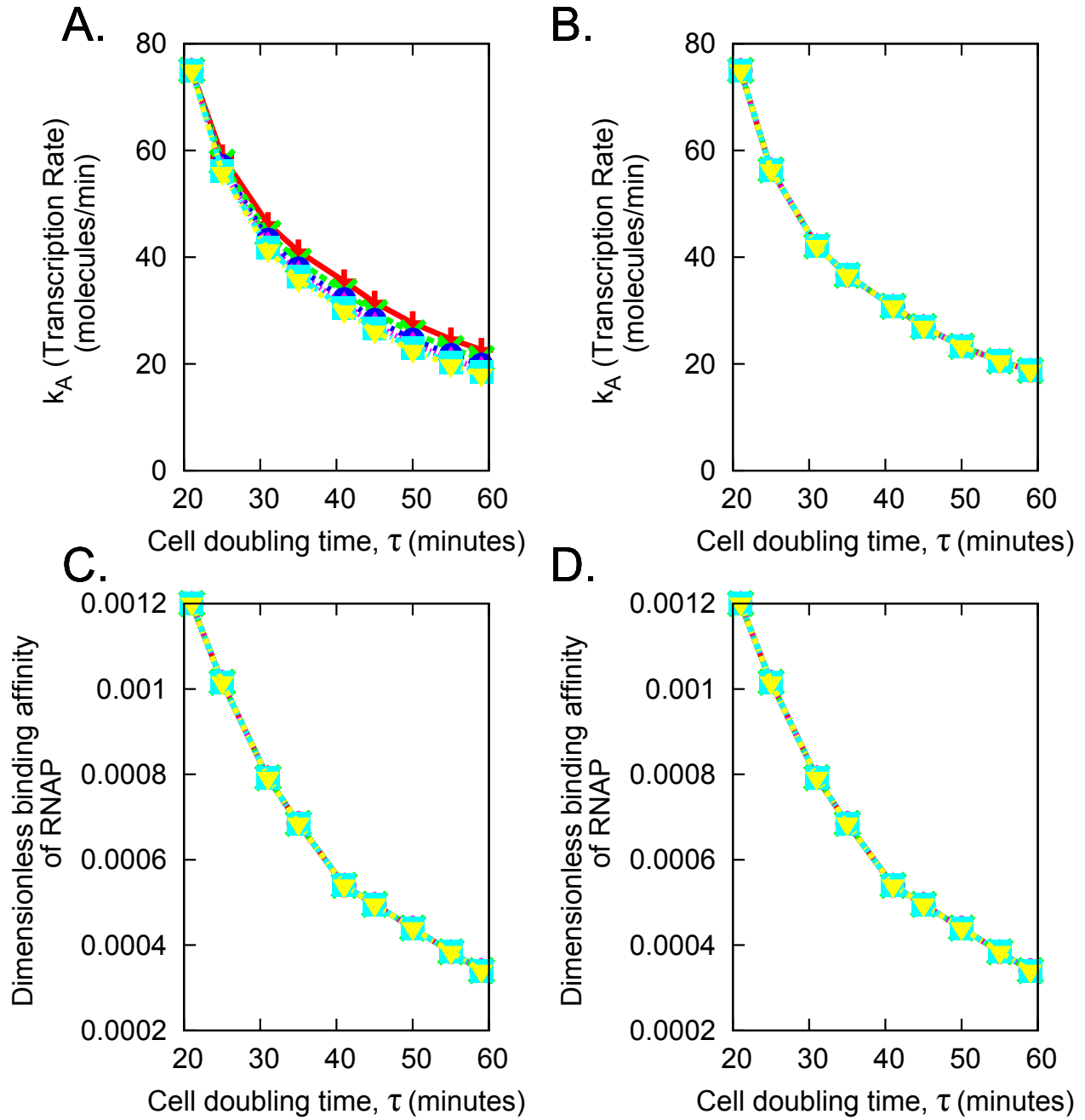


Figure A9: **The model with no autorepression but with RIDA is robust to changes in the input parameters.** A: The trend of k_A as the dimensionless binding affinity of RNAP to the DnaA promoter is varied. B: The trend of k_A as the RIDA rate, k_R is varied. C: The trend of the dimensionless binding affinity of RNAP to the DnaA promoter as k_A is varied. D: The trend of the dimensionless binding affinity of RNAP to the DnaA promoter as the RIDA rate, k_R is varied. In each case, the set different values taken by the varied parameter, and the corresponding symbols in the plots, are the same as those given in the caption of Additional Figure A8.

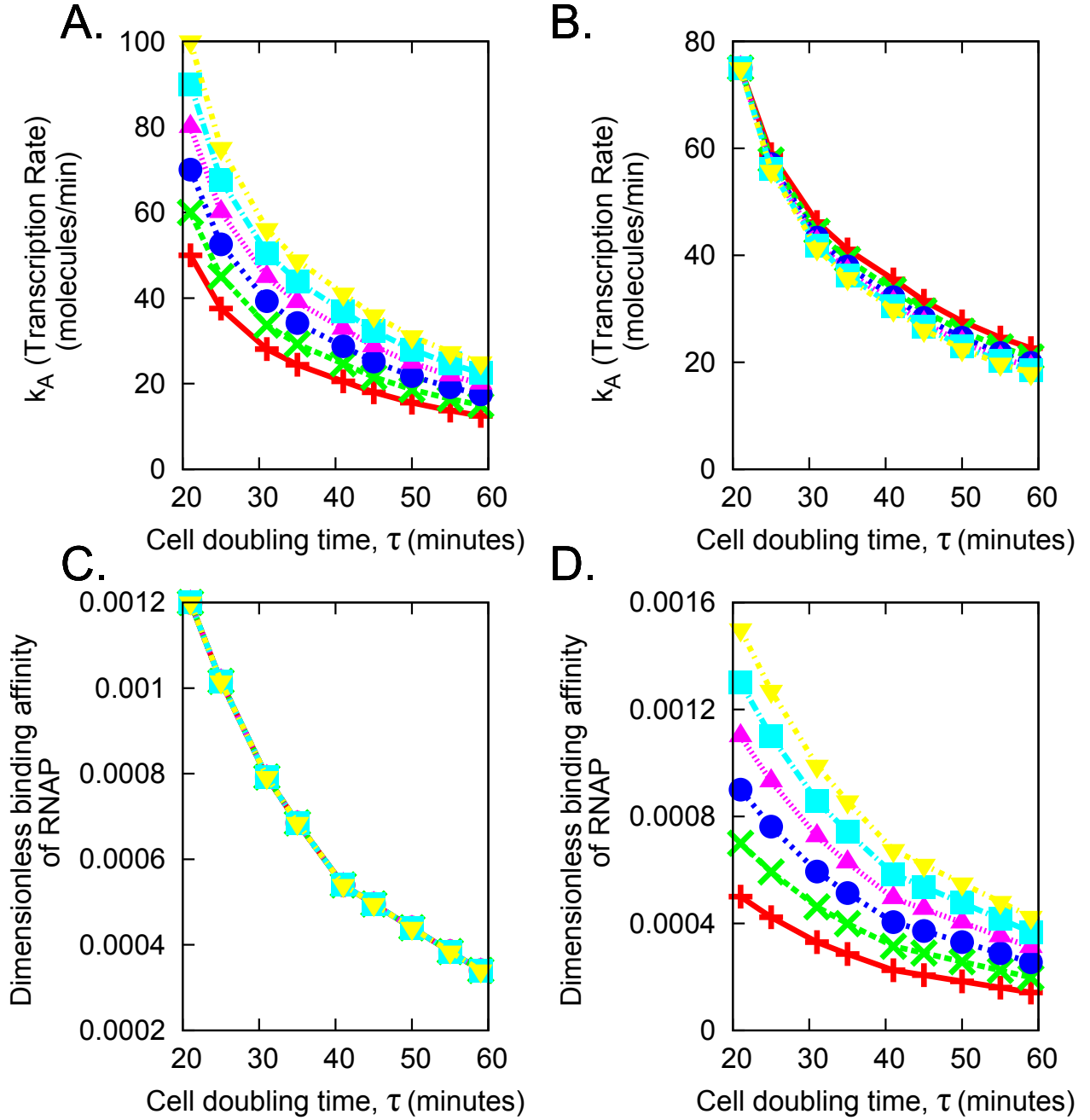


Figure A10: **The model with no autorepression and no RIDA is robust to changes in the input parameters.** A: The trend of k_A as the input value of k_A is varied. B: The trend of k_A as the dimensionless binding affinity of RNAP to the DnaA promoter is varied. C: The trend of the dimensionless binding affinity of RNAP to the DnaA promoter as k_A is varied. D: The trend of the dimensionless binding affinity of RNAP to the DnaA promoter is varied. In each case, the set different values taken by the varied parameter, and the corresponding symbols, are the same as those given in the caption of Figure A8. Note that the spread seen in A and D is due to the fact that these plots are relative to parameters whose initial values (at $\tau = 21$ mins) are themselves changed. The observation that the transformation makes the initial spread at $\tau = 60$ mins narrower for larger τ is further evidence of robustness.

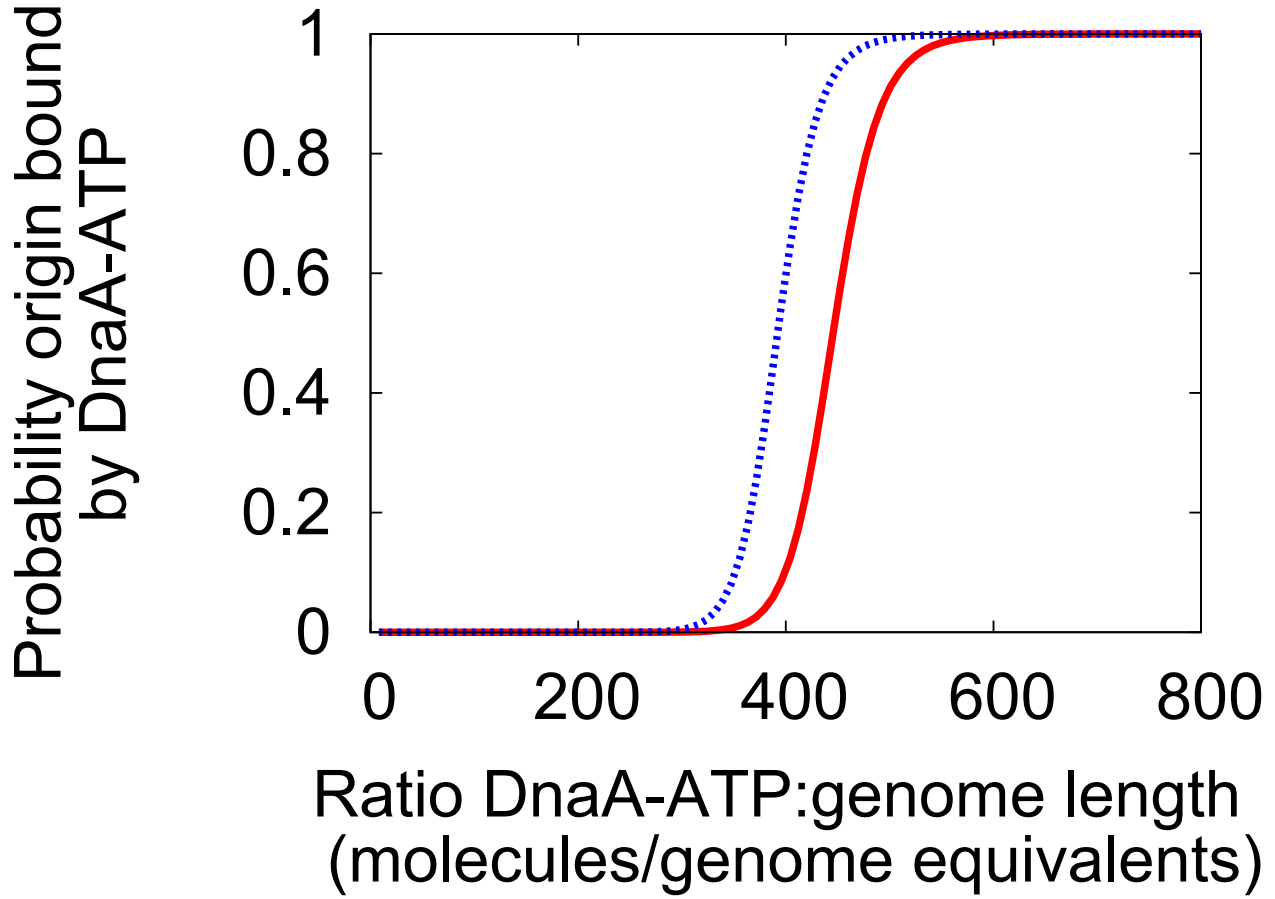


Figure A11: **Varying the binding affinity of DnaA-ATP to the sites at the origin has only a minor effect on the initiation threshold.** The probability of twenty DnaA-ATP molecules binding to the promoter, and hence starting initiation (as given in equation (26)) was plotted for different values of the binding affinity $e^{\Delta\epsilon_{ao}/k_B T}$, to examine whether this had a large effect on the initiation threshold. The values chosen for the binding affinity were $e^{\Delta\epsilon_{ao}/k_B T} = 0.0001$ (solid red curve), and $e^{\Delta\epsilon_{ao}/k_B T} = 0.000088$ (dashed blue curve), which are the extreme values that the binding affinity of DnaA-ATP to its self repression sites attains in Scenario 1a (see Figure 4). The initiation threshold is given by the inflection point of the curve. Thus, the difference between the initiation thresholds is ≈ 40 (molecules/genome equivalents) $\approx 10\%$ change. This is approximately constant, particularly when compared with the differences in $r(X)$ attained in the untransformed model (Figure 3A), suggesting that this scenario might be robust.